INTERNATIONAL ATOMIC ENERGY AGENCY
UNITED NATIONS EDUCATIONAL, SCIENTIFIC AND CULTURAL ORGANIZATION
INTERNATIONAL CENTRE FOR THEORETICAL PHYSICS
I.C.T.P,P.O. BOX 586,34100 TRIESTE,ITALY,CABLE:CENTRATOM TRIESTE

H4-SMR 1012 - 33

AUTUMN COLLEGE ON PLASMA PHYSICS

13 October - 7 November 1997

ELECTRON SCATTERING AND LOSS FROM THE INNER MAGNETOSPHERE

R.M. THORNE

UCLA, Los Angeles, U.S.A.

These are lecture notes, intended for distribution to participants.

MAIN BUILDING STRADA COSTIERA, 11 TEL. 22401 TELEFAX 224163 TELEX 460392 ADRIATICO GUEST HOUSE VIA GRIGNANO, 9 TEL. 224241 TELEFAX 224531 TELEX 460449
MICROPROCESSOR LAB. VIA BEIRUT, 31 TEL. 224471 TELEFAX 224463 TELEX 460392 GALILEO GUEST HOUSE VIA BEIRUT, 7 TEL. 22401 TELEFAX 224559 TELEX 460392

Electron Scattering and Loss from the Inner Magnetosphere.

R. M. Thorne UCLA

B. Abel Olympic College, WA.

1. Review of Adiabatic Motion
2. Non Adiabatic Processes: Injection and loss from the Radiation Belts
3. Resonant Wave-Particle Scattering
4. Equilibrium Pitch-Angle Distributions
5. Electron Lifetimes: Dominant Waves

Geomagnetic Trapping :

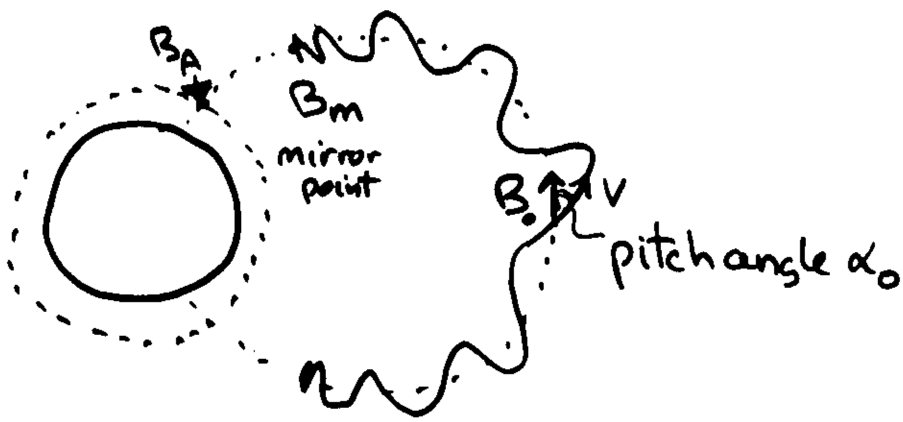

Conservation of 1st invariant $\mu = E_\perp / B \Rightarrow$ $\boxed{\dfrac{\sin^2\alpha_0}{B_0} = \text{const.} = \dfrac{1}{B_m}}$

Loss Cone : due to collisions in atmosphere below a critical altitude ($\lesssim 100$ km)

For $\alpha < \alpha_L$ such that $\boxed{\dfrac{\sin^2\alpha_L}{B_0} = \dfrac{1}{B_A}}$

the particle mirror point will lie below the top of the atmosphere! Such particles will be removed by collisions. Generally the loss cone will be empty. $\boxed{f(\alpha < \alpha_L) \Rightarrow 0}$

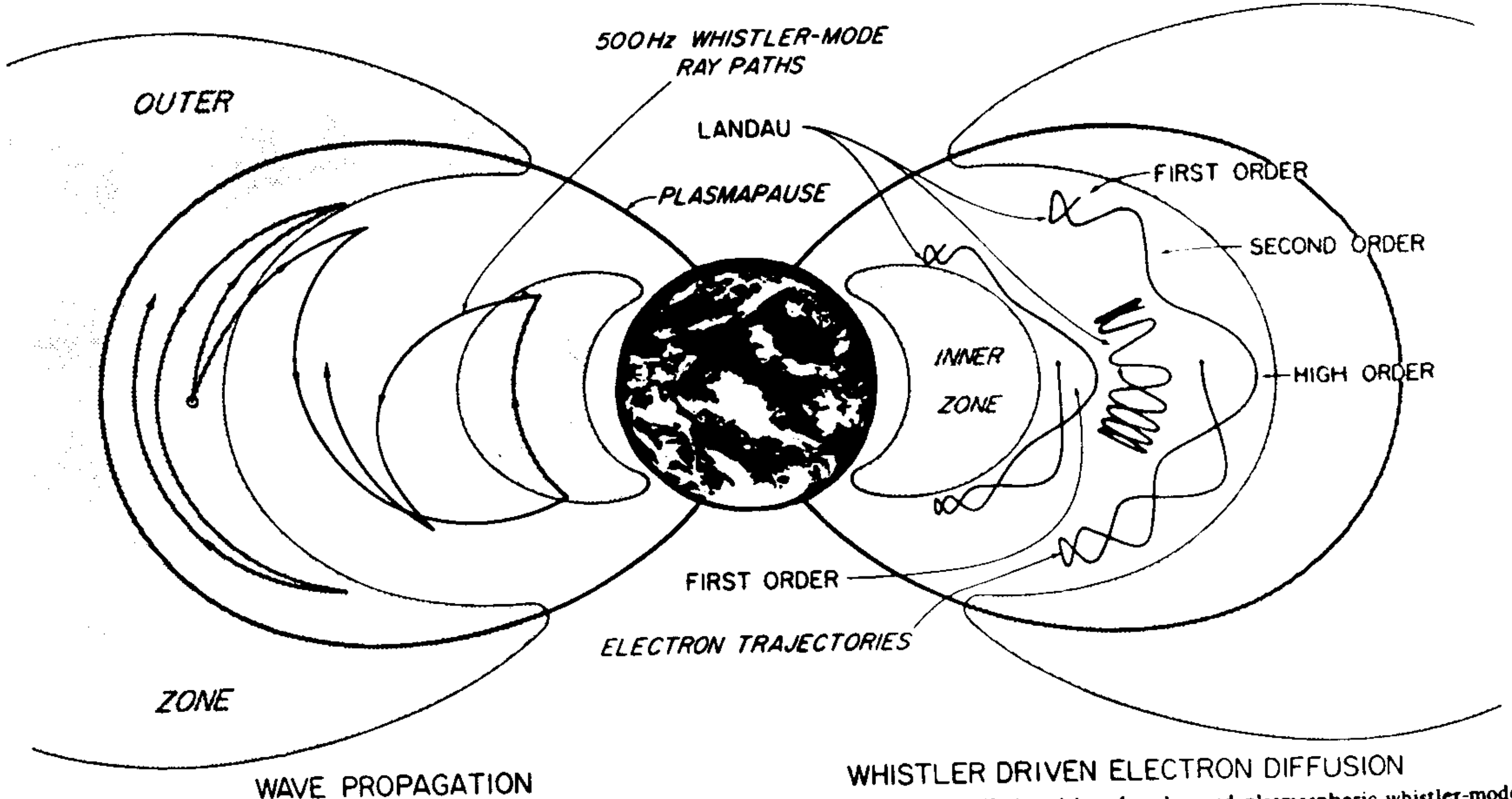

Fig. 3. Illustration of plasmaspheric whistler-mode wave propagation and electron pitch angle diffusion driven by observed plasmaspheric whistler-mode hiss (from Lyons *et al.*, 1972). The left-hand side of the figure shows examples of 500 Hz whistler-mode ray paths (obtained using the Stanford ray tracing program) which illustrate how waves generated near the plasmapause can propagate so as to fill the plasmasphere. The right-hand side of the figure illustrates the parasitic resonant interactions that occur between the plasmaspheric wave band and radiation belt electrons along three typical magnetospheric electron trajectories. Electrons near the inner edge of the slot (inner trajectory) are diffused primarily by first-order cyclotron resonance encountered near the equator. The diffusion of electrons in the outer regions of the slot (outer trajectory) is controlled by the combination of first order cyclotron resonance at high latitudes and higher harmonic resonances at lower latitudes. All radiation belt electrons encounter the Landau resonance near the mirror points, however such diffusion is most important for electrons of high equatorial pitch angles (middle trajectory).

Lyons, Thorne, Kennel : JGR, '72

The rate of Pitch-Angle Scattering by Waves.

Under pure pitch-angle scattering (no energy change) the particle distribution function is controlled by:

$$\frac{\partial f}{\partial t} = \frac{1}{\sin\alpha}\frac{\partial}{\partial \alpha}\left(D_{\alpha\alpha}\frac{\partial f}{\partial \alpha}\right) + S - L$$

loss

Rate of Diffusion ($D_{\alpha\alpha}$) — Source (S)

$$D_{\alpha\alpha} = \frac{\langle(\Delta\alpha)^2\rangle}{2\Delta t}$$

← This is controlled by the wave Power Spectral Density $P(\omega,k)$ and the order of resonance.

$$D_{\alpha\alpha} \sim B_{wave}^2$$

The theoretical formalism to compute $D_{\alpha\alpha}$ has been described by Lyons, Thorne, Kennel; JGR, 77, 3455, 1972.

To utilize this for geomagnetically trapped electrons the rate of scattering must first be averaged over the particle's bounce orbit. Numerical calculations of $\mathcal{D}(\alpha_0)$ can then be used to calculate the particle lifetime τ_c and the equilibrium distribution function $f(\alpha_0)$ of electrons.

Since Coulomb lifetimes are <u>very</u> long for high energy electrons, wave scattering can be a dominant loss process.

Bounced Averaged Rate of Scattering.

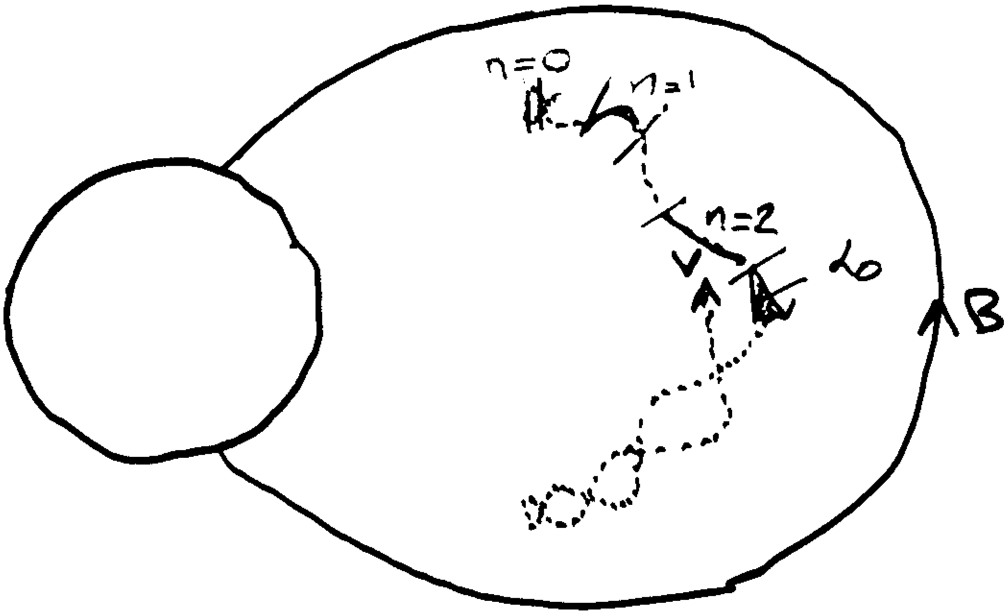

① Classify each electron in terms of α_0 at $\underline{\lambda = 0}$.

② Determine latitude range along bounce orbit for each harmonic resonance ($n = 0, 1, 2 \ldots$ etc) and evaluate $D_{\alpha\alpha}(\lambda)$ for all resonant waves.

③ Obtain bounce orbit averaged diffusion rate

$$\mathcal{D}(\alpha_0) = \frac{1}{\tau_B} \int_0^{\tau_B} D(t) \left(\frac{\partial \alpha_0}{\partial \alpha}\right)^2 dt$$

Bounce orbit.

$$\boxed{\mathcal{D}(\alpha_0) = \frac{1}{T(\alpha_0)} \int_0^{\lambda_m} D(\alpha(\lambda)) \frac{\cos\alpha}{\cos^2\alpha_0} \cos^7\lambda \, d\lambda.}$$

$T(\alpha_0) \simeq 1.3 - 0.56 \sin\alpha_0$: $\quad \boxed{\dfrac{\sin^2\alpha(\lambda)}{B(\lambda)} = \dfrac{\sin^2\alpha_0}{B_0}}$

variation of T_B with α_0

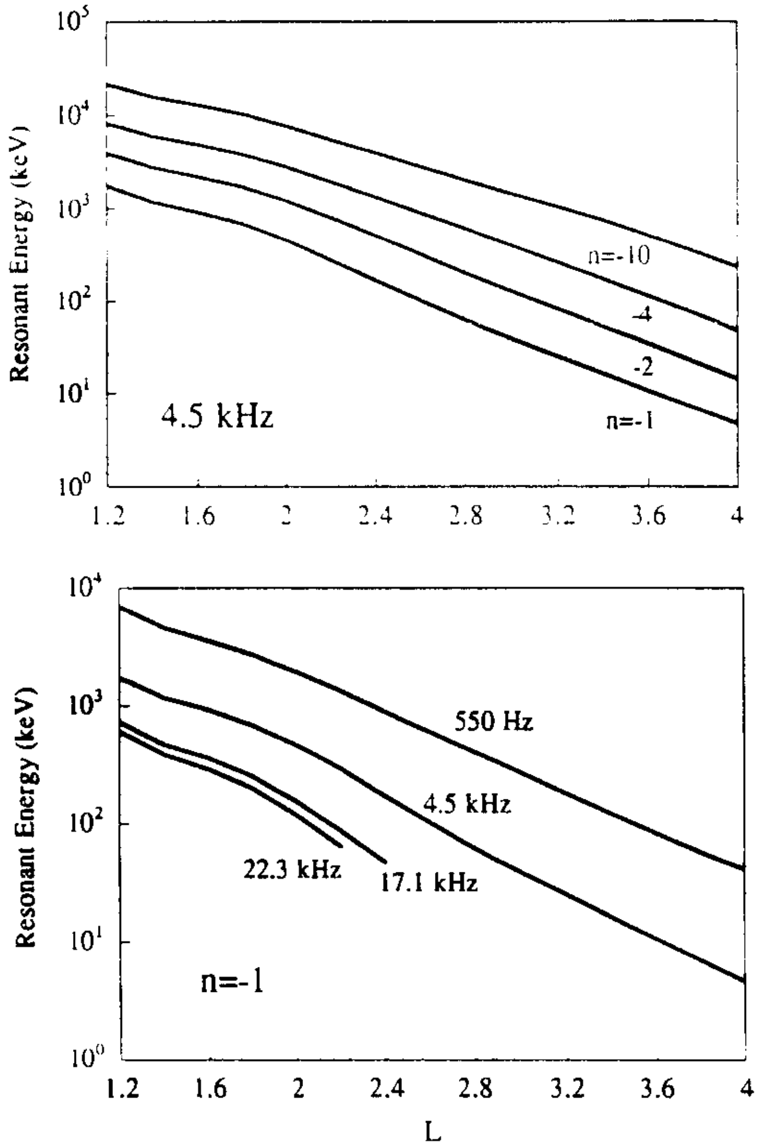

Resonant Energy (keV)
4.5 kHz
n=-10
-4
-2
n=-1
Resonant Energy (keV)
550 Hz
4.5 kHz
22.3 kHz
17.1 kHz
n=-1
L

Fig 2

Bounce Averaged $\mathcal{D}(\alpha_0)$ for plasmaspheric Hiss in the outer plasmasphere.

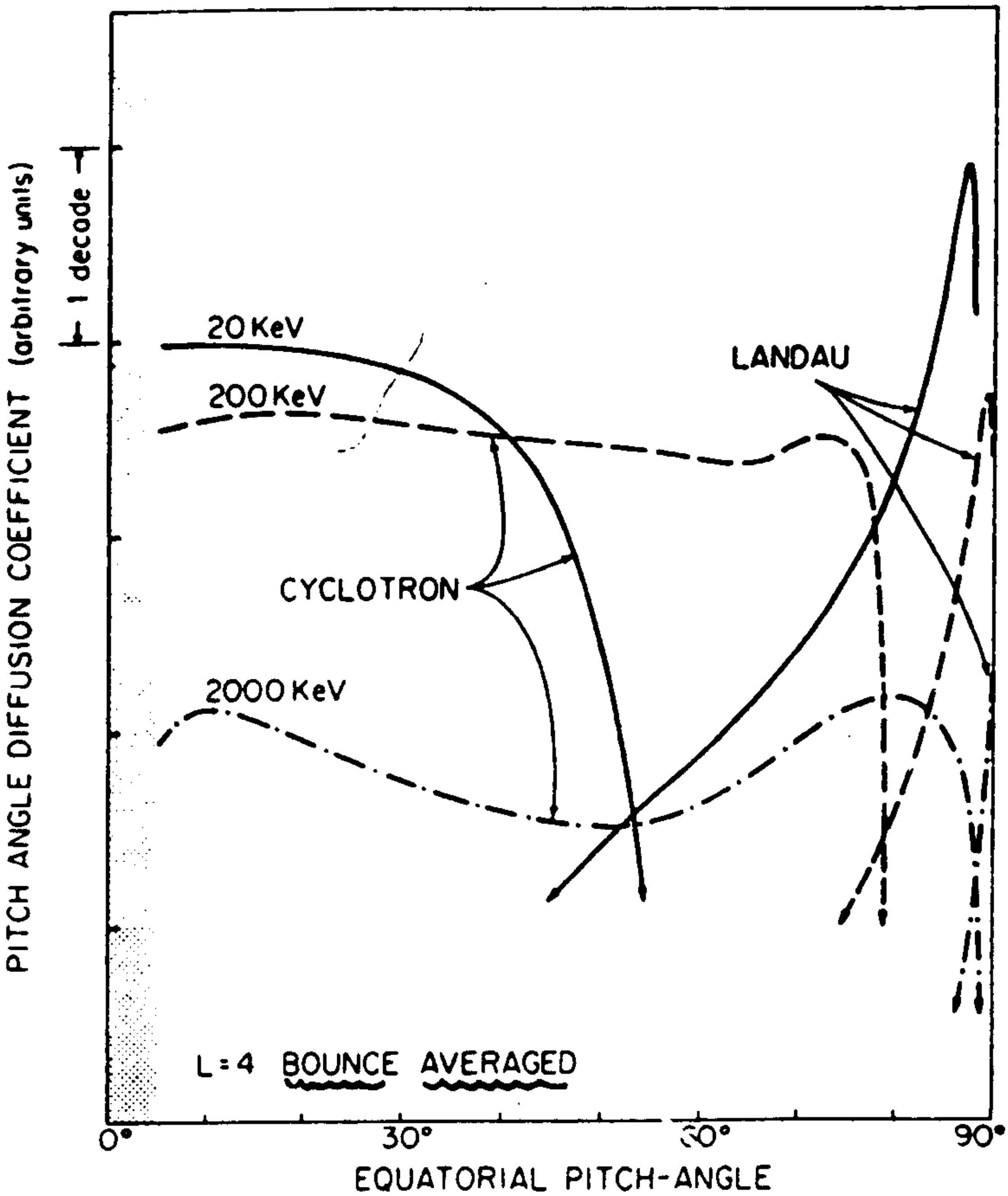

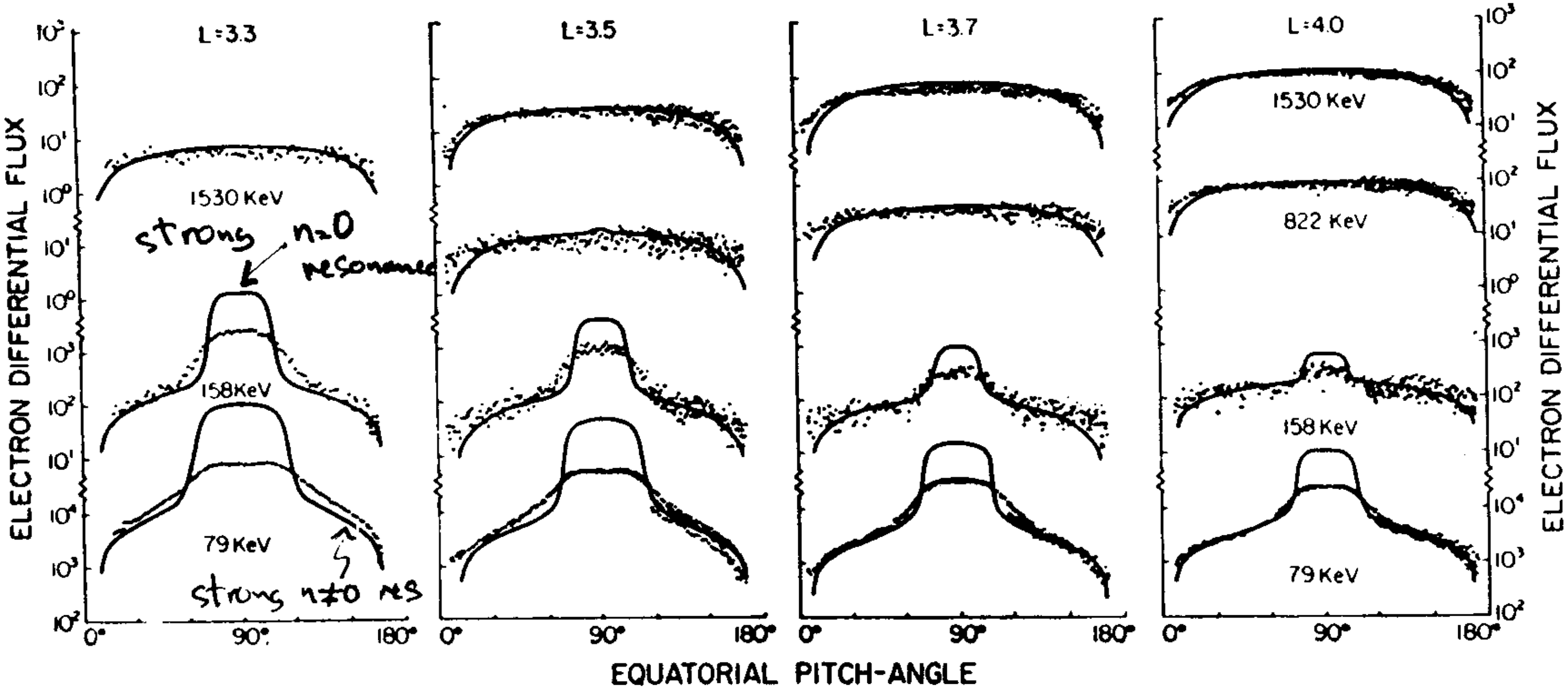

Fig. 6. Comparison of calculated equatorial pitch-angle distributions with equatorial distributions observed within the electron slot during the decay phase following an injection event (West, personal communication, 1971). The data points (electrons/cm²-sec-ster-kev) are plotted as a function of pitch angle at the L values and energies indicated on the figure. The vertical positionings of the corresponding calculated distributions, shown by solid lines, are arbitrary on a logarithmic scale and have therefore been adjusted so as to best fit the data.

Lyons et al 77, 3455, 1972.

Wave Parameters

Type of Wave	Plasmaspheric Hiss	Lightning-Generated Whistlers	VLF Transmitters
Frequency	550±300 Hz	4.5±2 kHz	17.1 kHz ± 50 Hz and 22.3 kHz ± 50 Hz
Propagation Angle	45° ± 22.5°	45° ± 22.5°	45° ± 22.5°
Wave Intensity	10 mγ	10 mγ	Variable
Occurrence Rate	10% for L<2 (Tsurutani et al) ramps linearly to 50% at L=3, 50% for L≥3 Russell et al.	3%	2.4% each

Electron Energy Range: 100-1,500 keV

Multi-Species Density Calculations:
- Neutrals: MSIS90 [*Hedin*, 1991]
- Electrons: [*Chiu et al.*, 1979]
- Ions: IRI90 [*Rawer*, 1982] Anchored to Electrons

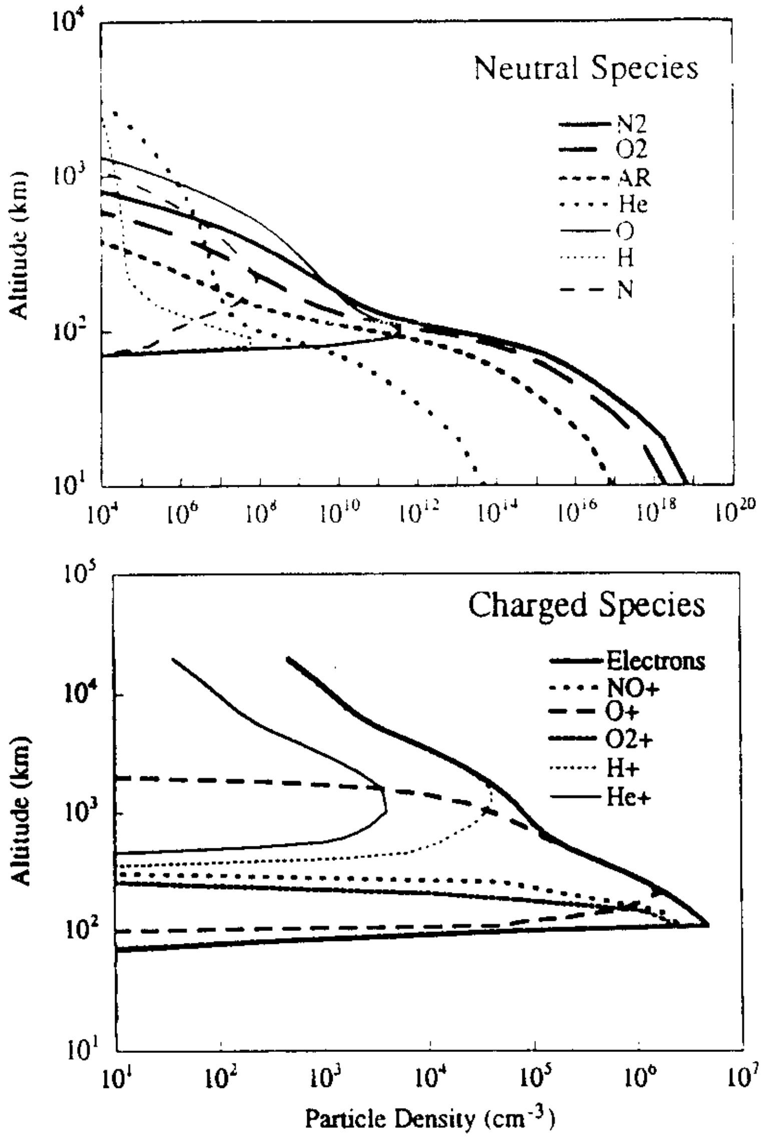

Neutral Species
N2
O2
AR
He
O
H
N
Altitude (km)
Charged Species
Electrons
NO+
O+
O2+
H+
He+
Altitude (km)
Particle Density (cm^{-3})

Fig. 1

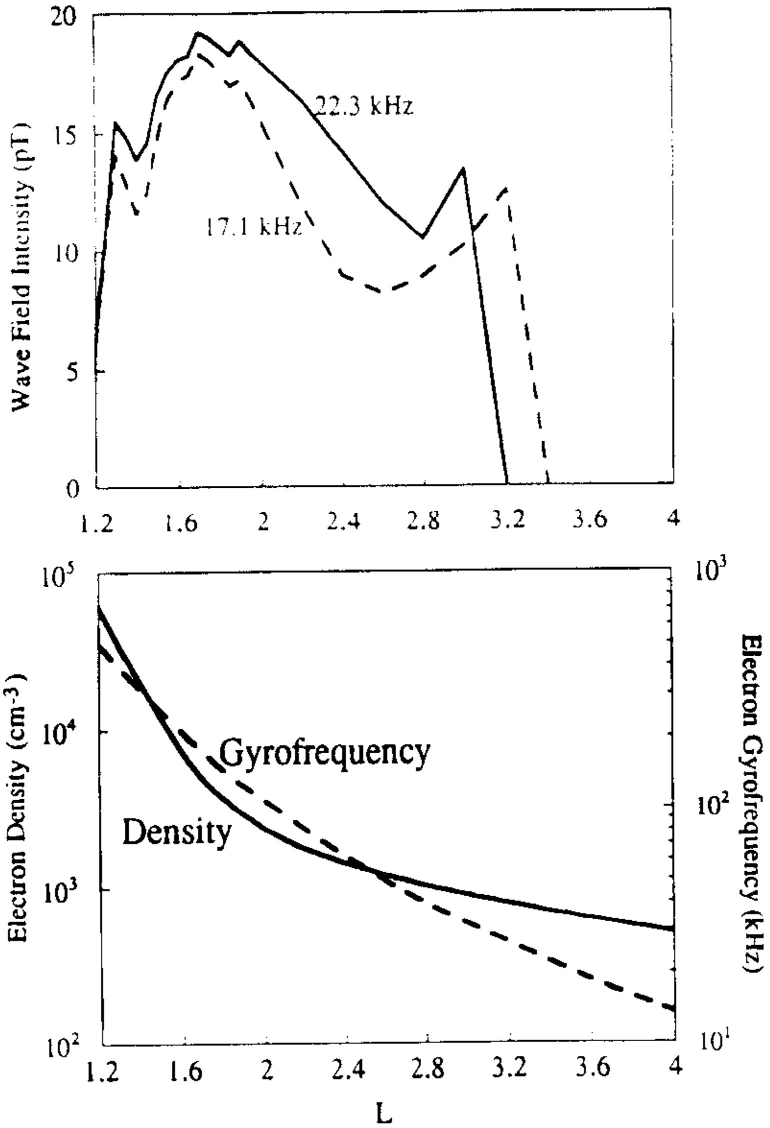

20
15
10
5
0
Wave Field Intensity (pT)
22.3 kHz
17.1 kHz
1.2
1.6
2
2.4
2.8
3.2
3.6
4
10^5
10^4
10^3
10^2
Electron Density (cm^{-3})
Gyrofrequency
Density
10^3
10^2
10^1
Electron Gyrofrequency (kHz)
1.2
1.6
2
2.4
2.8
3.2
3.6
4
L

Fig.

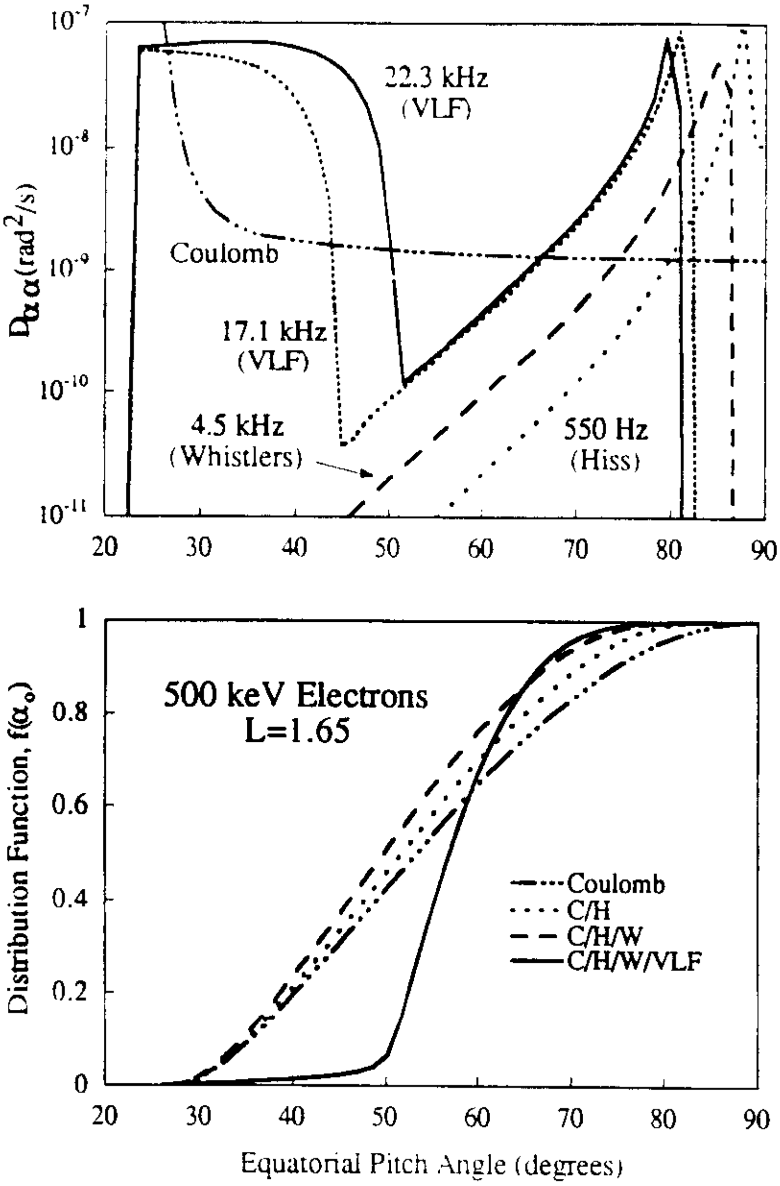

22.3 kHz
(VLF)
Coulomb
17.1 kHz
(VLF)
4.5 kHz
(Whistlers)
550 Hz
(Hiss)
$D_{\alpha\alpha}$ (rad^2/s)
500 keV Electrons
L=1.65
Coulomb
C/H
C/H/W
C/H/W/VLF
Distribution Function, $f(\alpha_o)$
Equatorial Pitch Angle (degrees)

Fig. 4

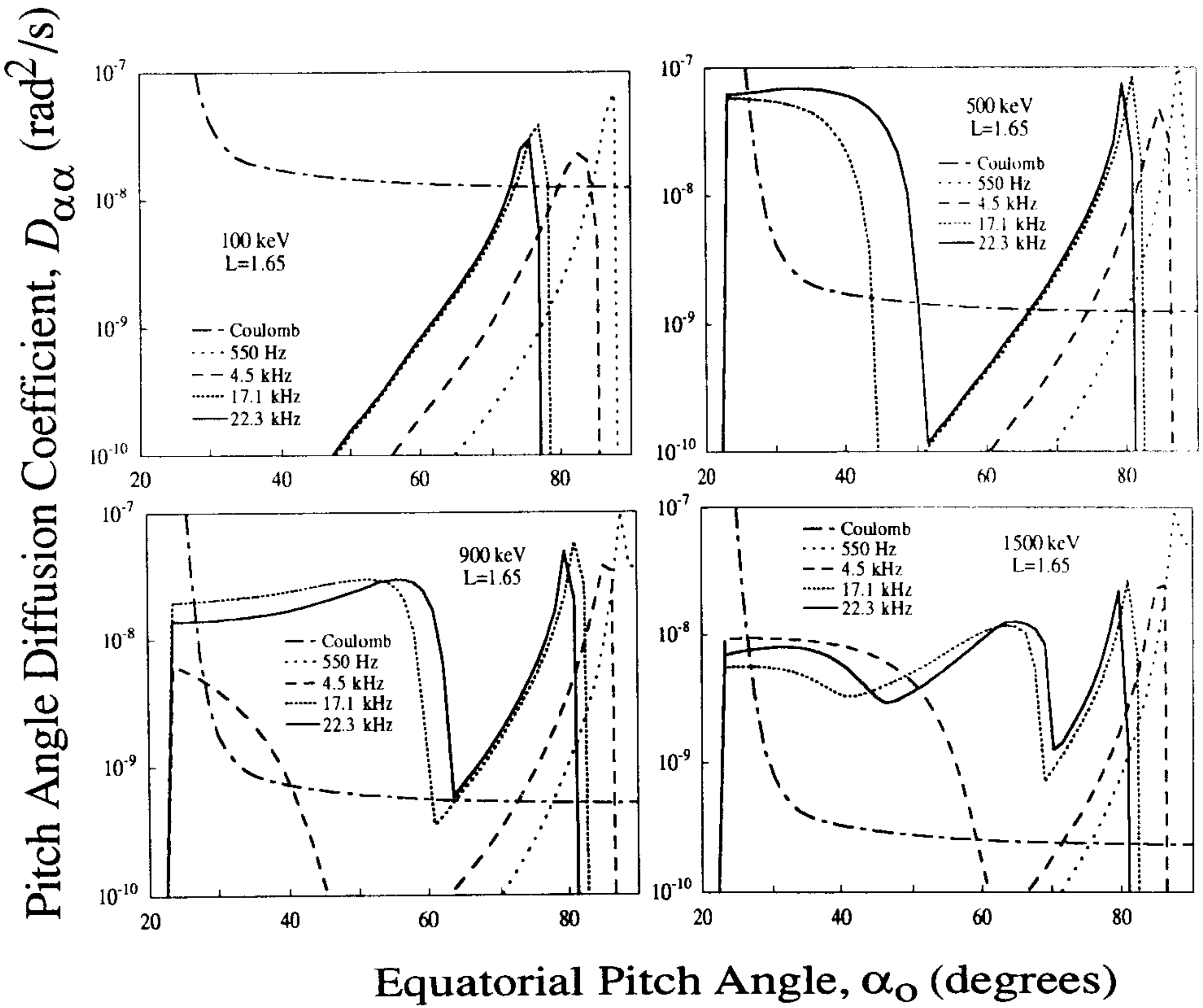
Pitch Angle Diffusion Coefficient, $D_{\alpha\alpha}$ (rad^2/s)
Equatorial Pitch Angle, α_o (degrees)
100 keV
L=1.65
500 keV
L=1.65
900 keV
L=1.65
1500 keV
L=1.65
Coulomb
550 Hz
4.5 kHz
17.1 kHz
22.3 kHz
10^{-7}
10^{-8}
10^{-9}
10^{-10}
20
40
60
80

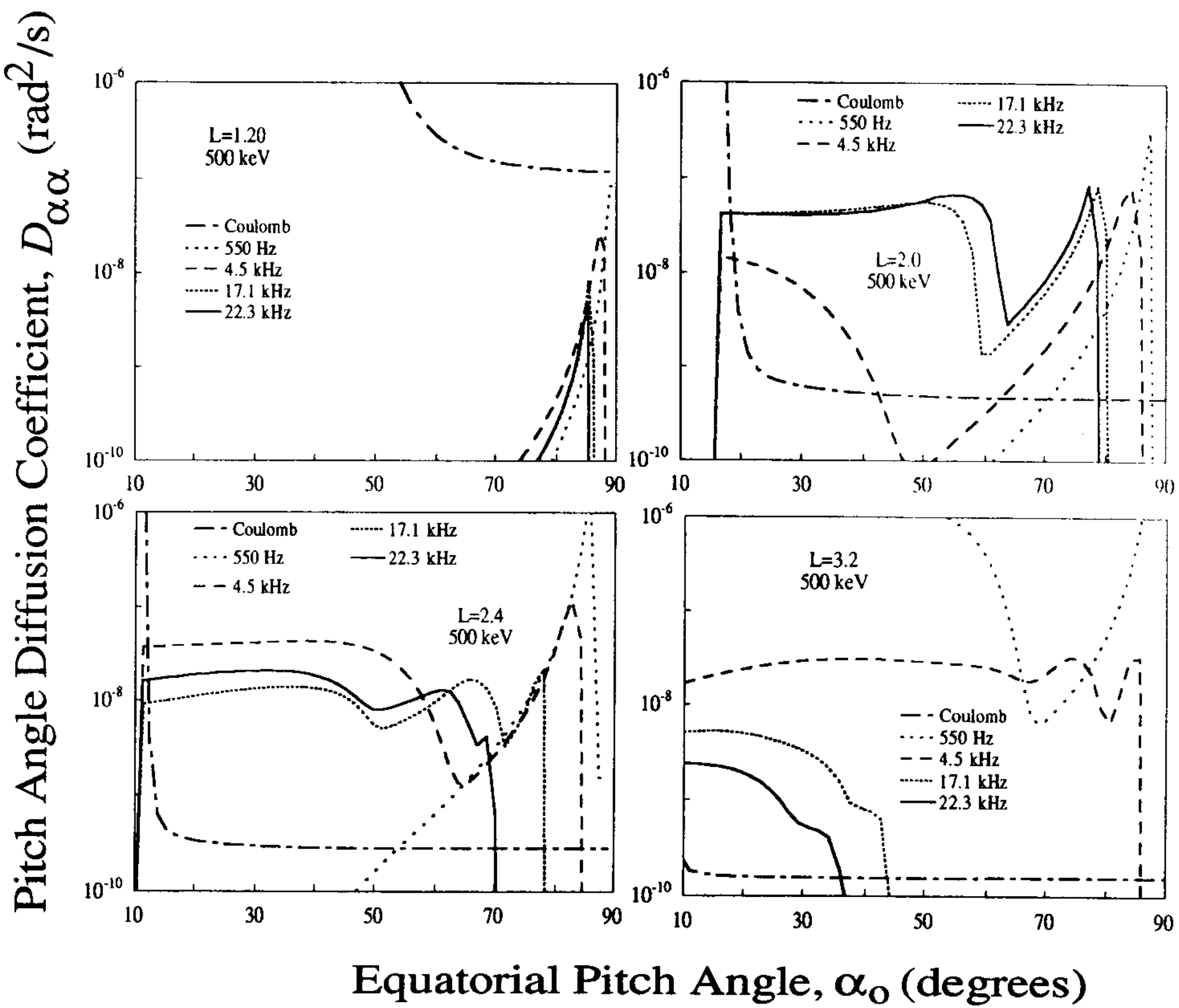

Pitch Angle Diffusion Coefficient, $D_{\alpha\alpha}$ (rad^2/s)
Equatorial Pitch Angle, α_o (degrees)
L=1.20
500 keV
L=2.0
500 keV
L=2.4
500 keV
L=3.2
500 keV
Coulomb
550 Hz
4.5 kHz
17.1 kHz
22.3 kHz
10^{-6}
10^{-8}
10^{-10}
10
30
50
70
90

Fig. 6

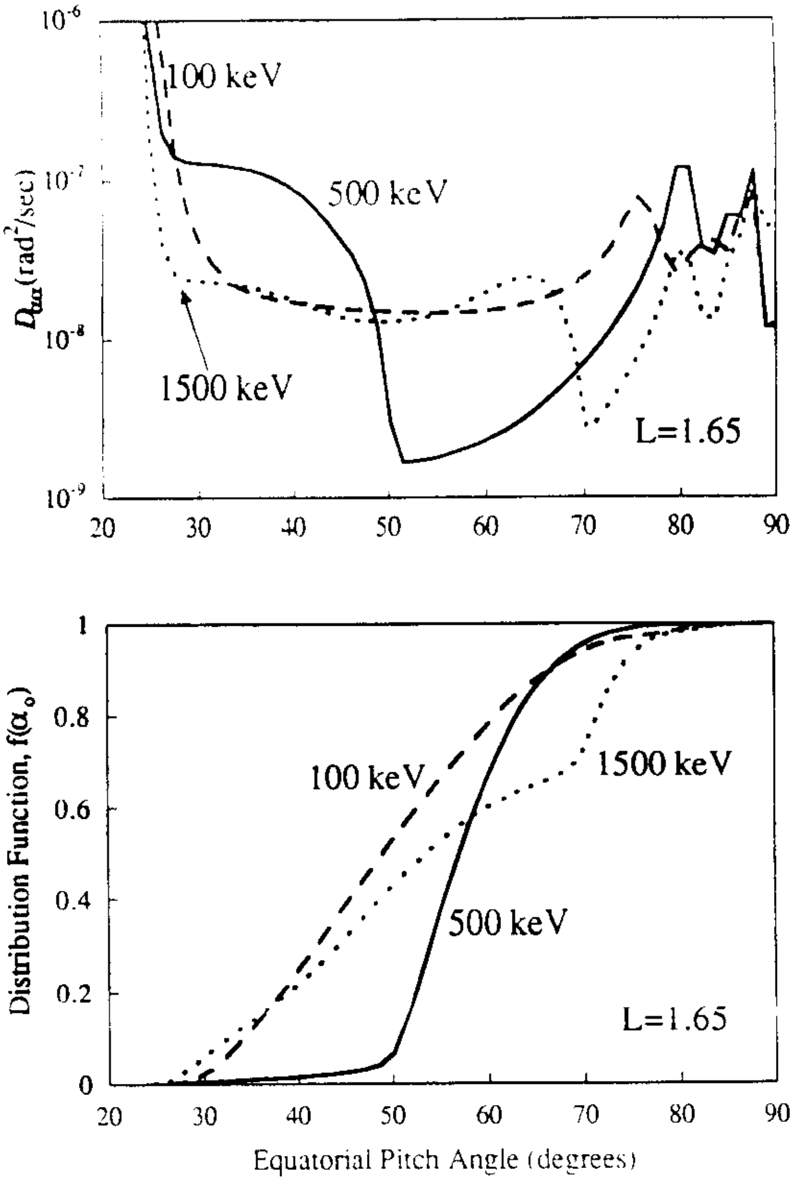

10^{-6}
10^{-7}
10^{-8}
10^{-9}
$D_{\alpha\alpha}$ (rad^2/sec)
100 keV
500 keV
1500 keV
L=1.65
20
30
40
50
60
70
80
90
1
0.8
0.6
0.4
0.2
0
Distribution Function, $f(\alpha_o)$
100 keV
1500 keV
500 keV
L=1.65
20
30
40
50
60
70
80
90
Equatorial Pitch Angle (degrees)

Fig. 7

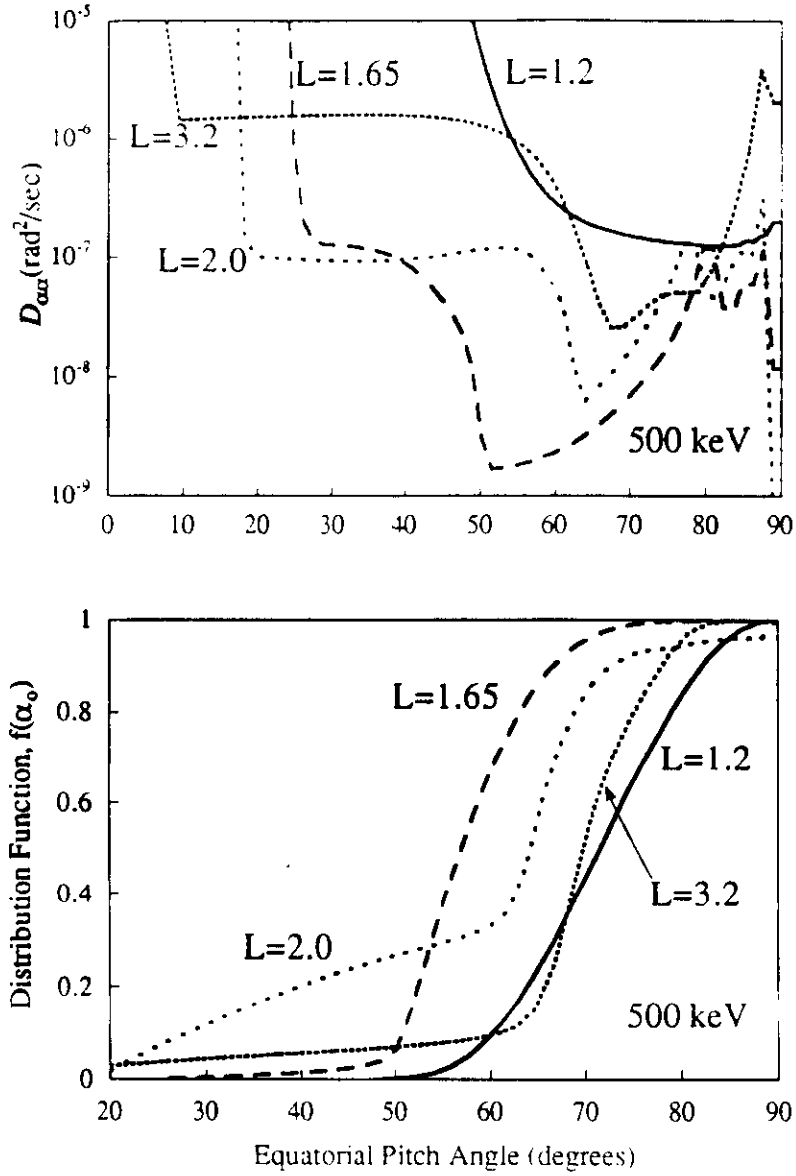
L=1.65
L=1.2
L=3.2
L=2.0
500 keV
$D_{\alpha\alpha}$(rad^2/sec)
10^{-5}
10^{-6}
10^{-7}
10^{-8}
10^{-9}
0 10 20 30 40 50 60 70 80 90
L=1.65
L=1.2
L=3.2
L=2.0
500 keV
Distribution Function, f(α_o)
1
0.8
0.6
0.4
0.2
0
20 30 40 50 60 70 80 90
Equatorial Pitch Angle (degrees)

Fg. i

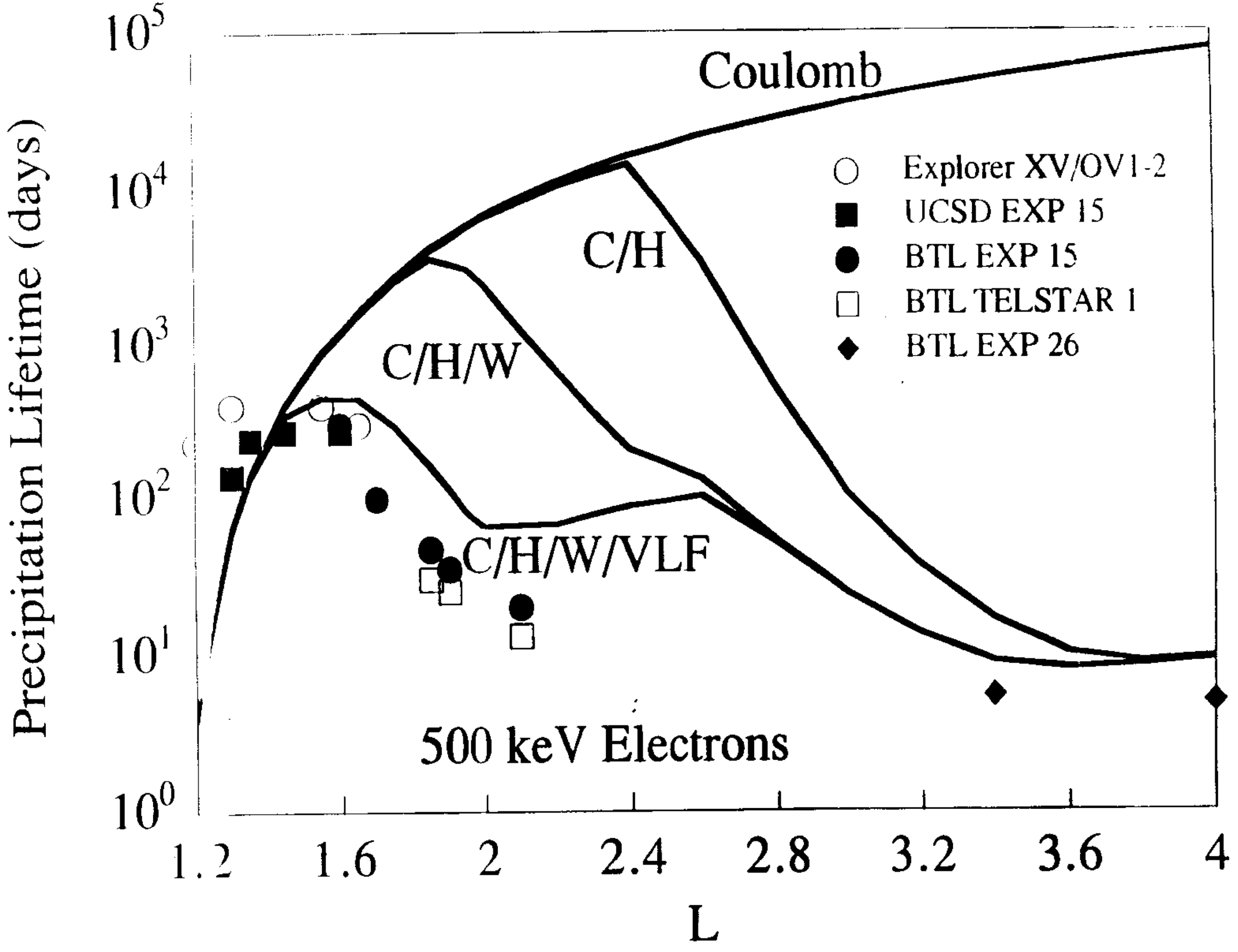

Precipitation Lifetime (days)
10^5
10^4
10^3
10^2
10^1
10^0
Coulomb
C/H
C/H/W
C/H/W/VLF
Explorer XV/OV1-2
UCSD EXP 15
BTL EXP 15
BTL TELSTAR 1
BTL EXP 26
500 keV Electrons
1.2
1.6
2
2.4
2.8
3.2
3.6
4
L

Fig.

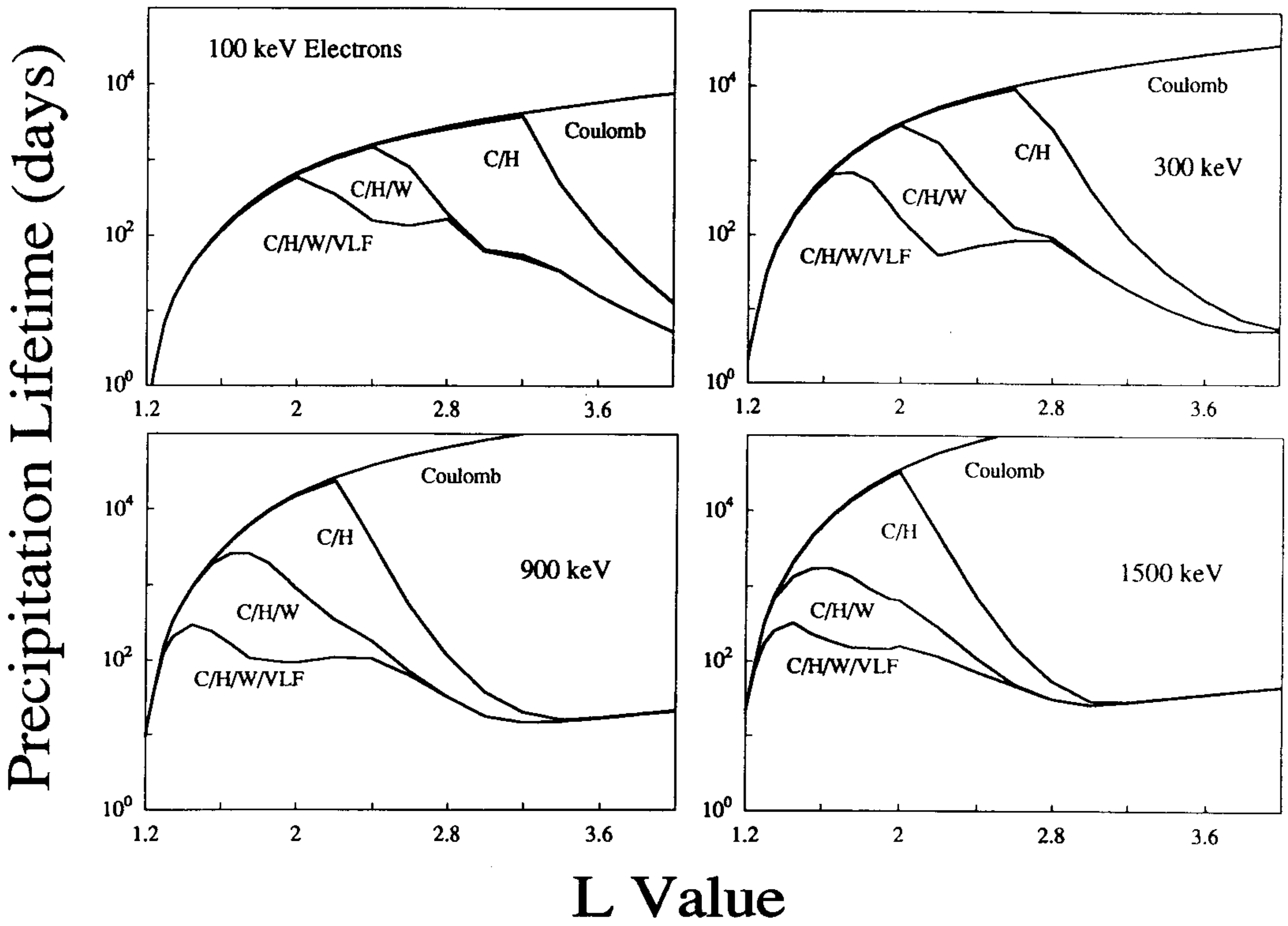
Precipitation Lifetime (days)
100 keV Electrons
Coulomb
C/H
C/H/W
C/H/W/VLF
300 keV
900 keV
1500 keV
10^0
10^2
10^4
1.2
2
2.8
3.6
L Value

Fig. 10

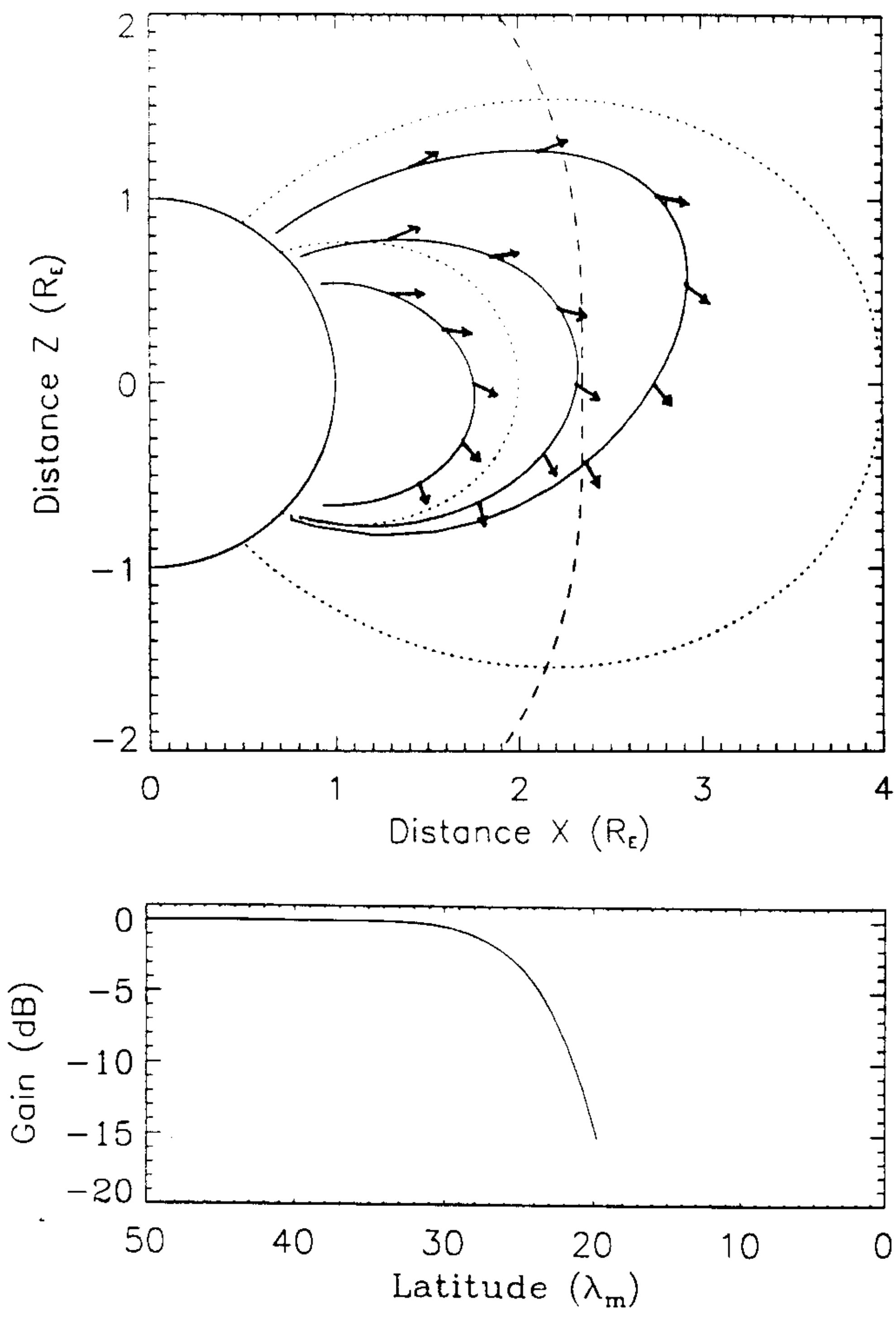

Fig. 1

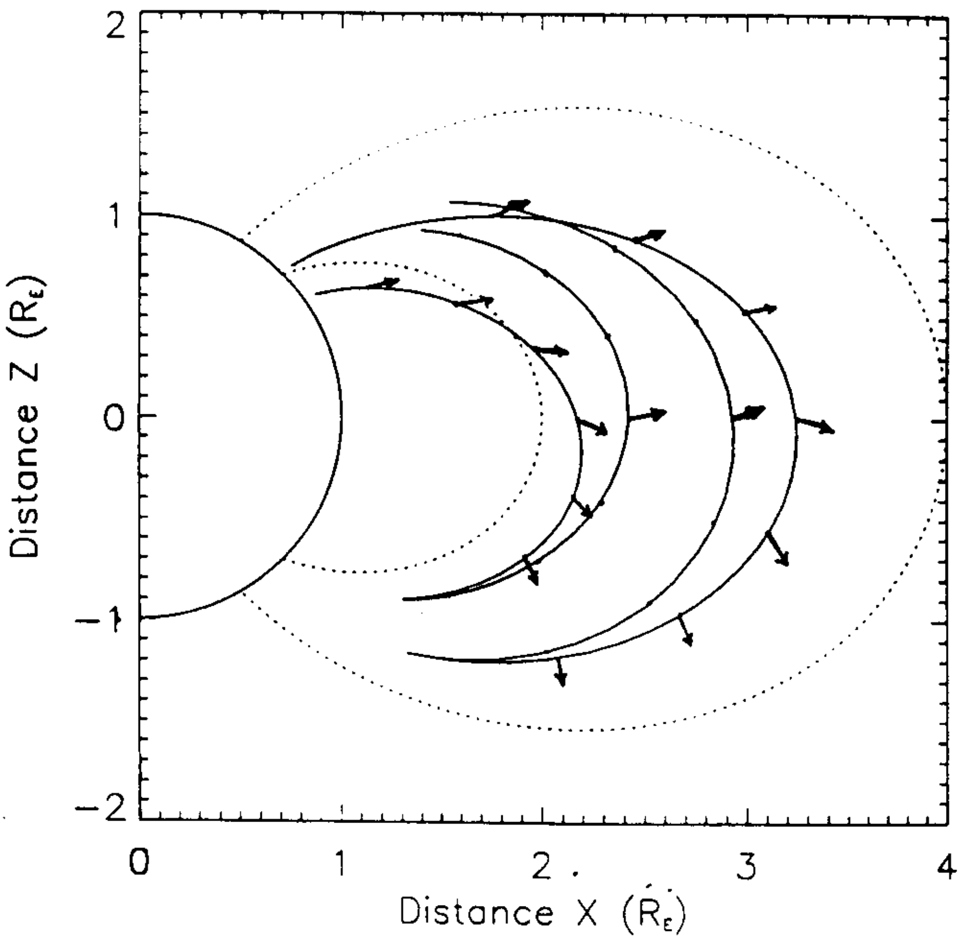

Fig. 2

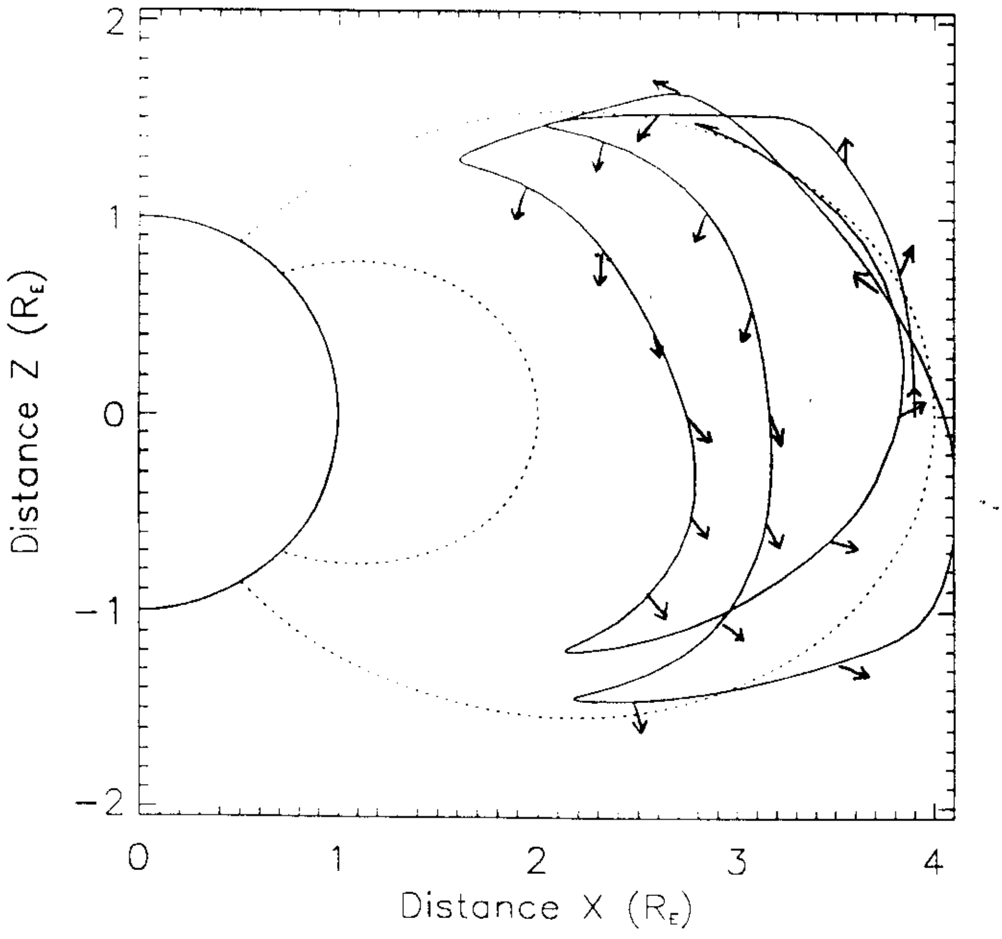

Fig. 3

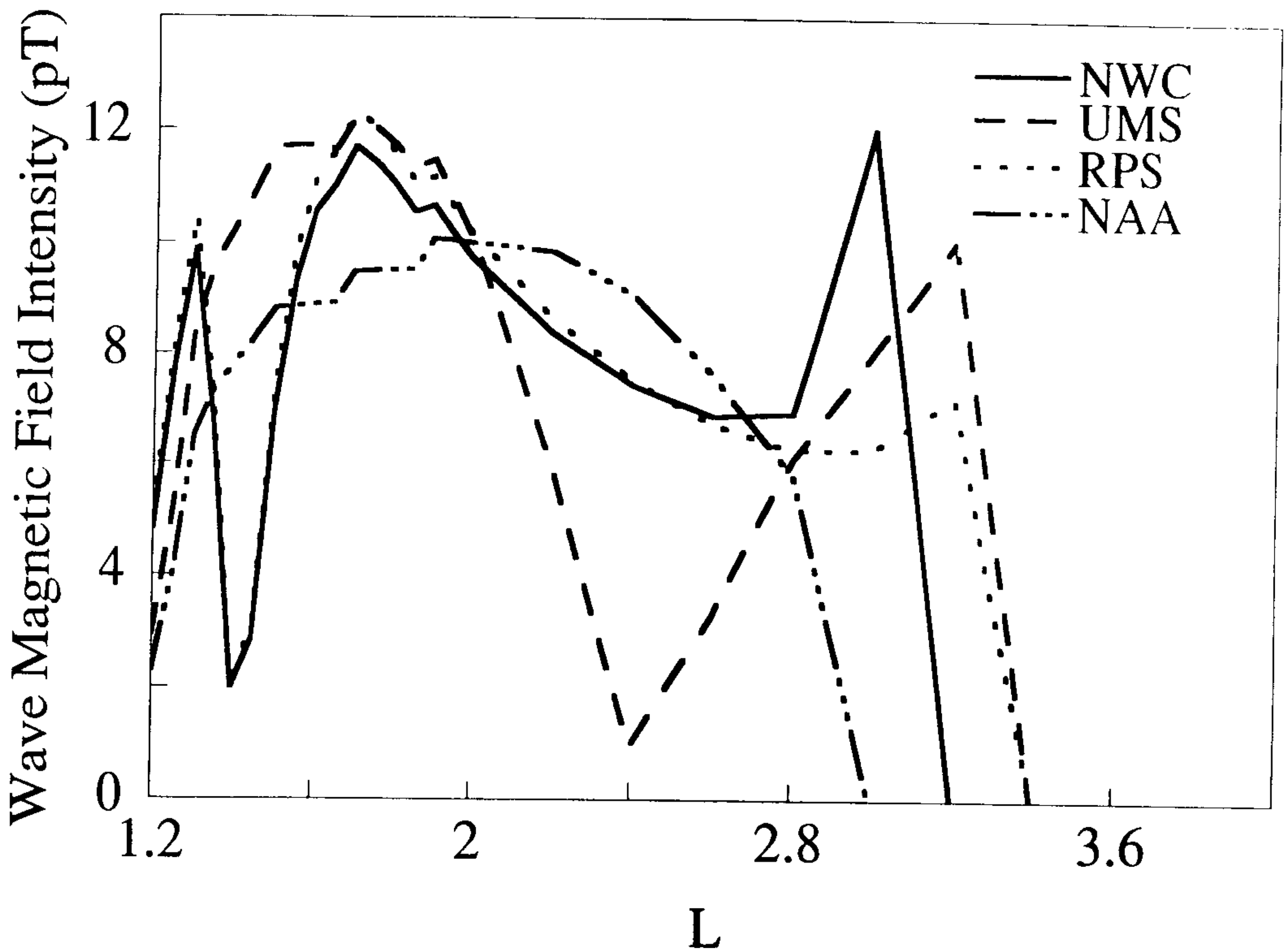
Wave Magnetic Field Intensity (pT)
0
4
8
12
1.2
2
2.8
3.6
L
NWC
UMS
RPS
NAA

Fig. 4

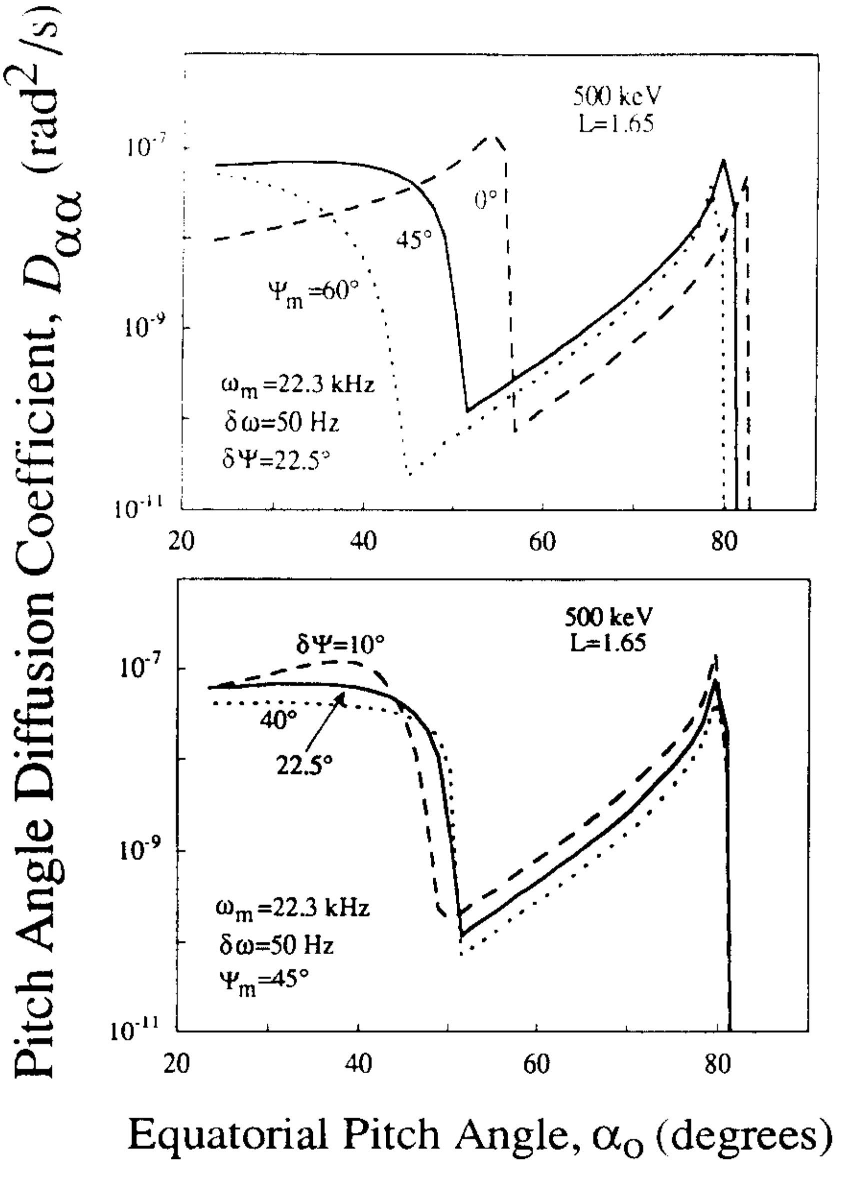

Pitch Angle Diffusion Coefficient, $D_{\alpha\alpha}$ (rad^2/s)
500 keV
L=1.65
0°
45°
Ψ_m=60°
ω_m=22.3 kHz
$\delta\omega$=50 Hz
$\delta\Psi$=22.5°
10^{-7}
10^{-9}
10^{-11}
20
40
60
80
500 keV
L=1.65
$\delta\Psi$=10°
40°
22.5°
ω_m=22.3 kHz
$\delta\omega$=50 Hz
Ψ_m=45°
Equatorial Pitch Angle, α_o (degrees)

Fig. 5

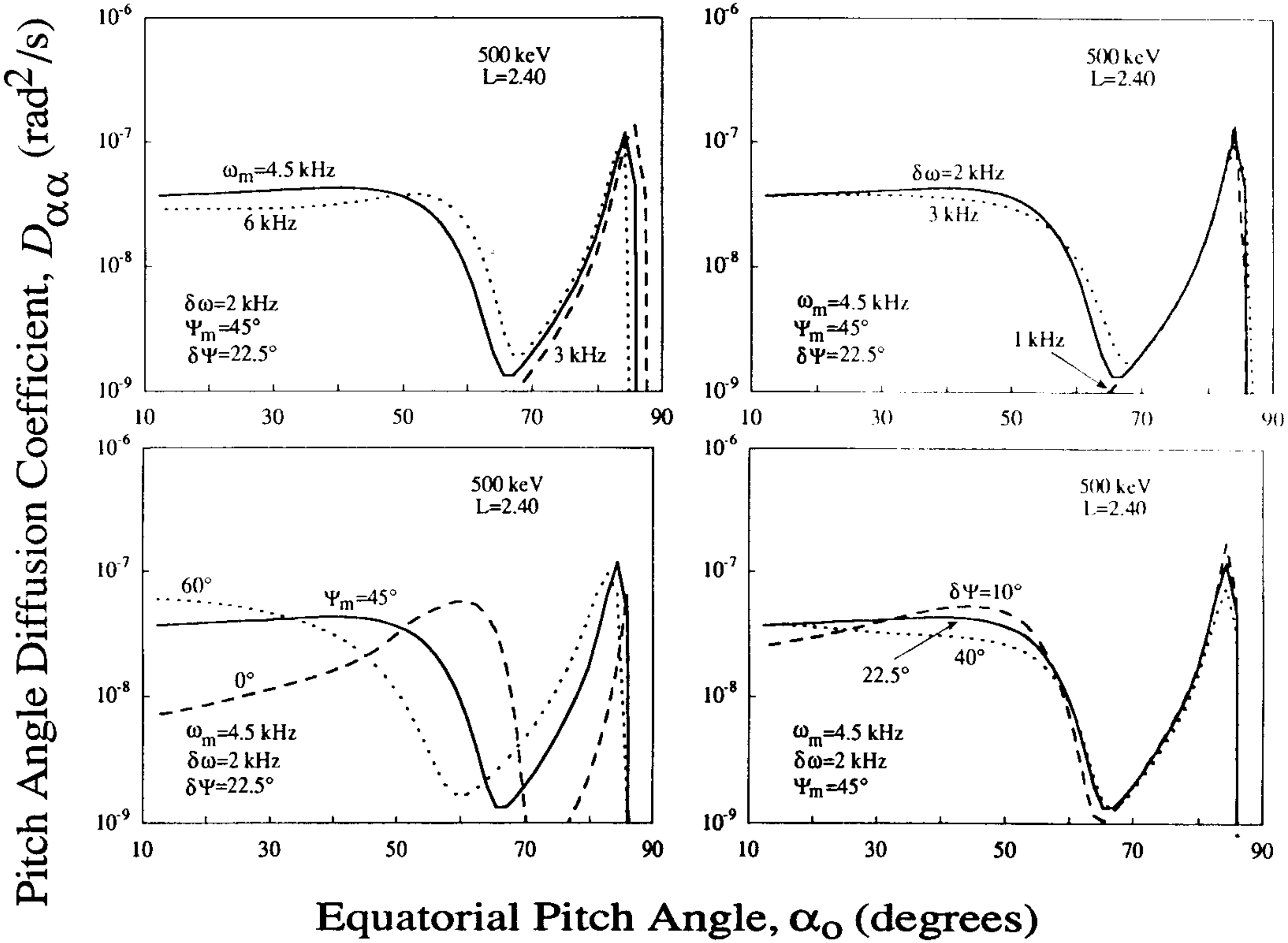

500 keV
L=2.40
ω_m=4.5 kHz
6 kHz
3 kHz
$\delta\omega$=2 kHz
Ψ_m=45°
$\delta\Psi$=22.5°
$\delta\omega$=2 kHz
3 kHz
1 kHz
ω_m=4.5 kHz
60°
Ψ_m=45°
0°
$\delta\Psi$=10°
22.5°
40°
10^{-6}
10^{-7}
10^{-8}
10^{-9}
10
30
50
70
90
Pitch Angle Diffusion Coefficient, $D_{\alpha\alpha}$ (rad^2/s)
Equatorial Pitch Angle, α_o (degrees)

Fig. 6

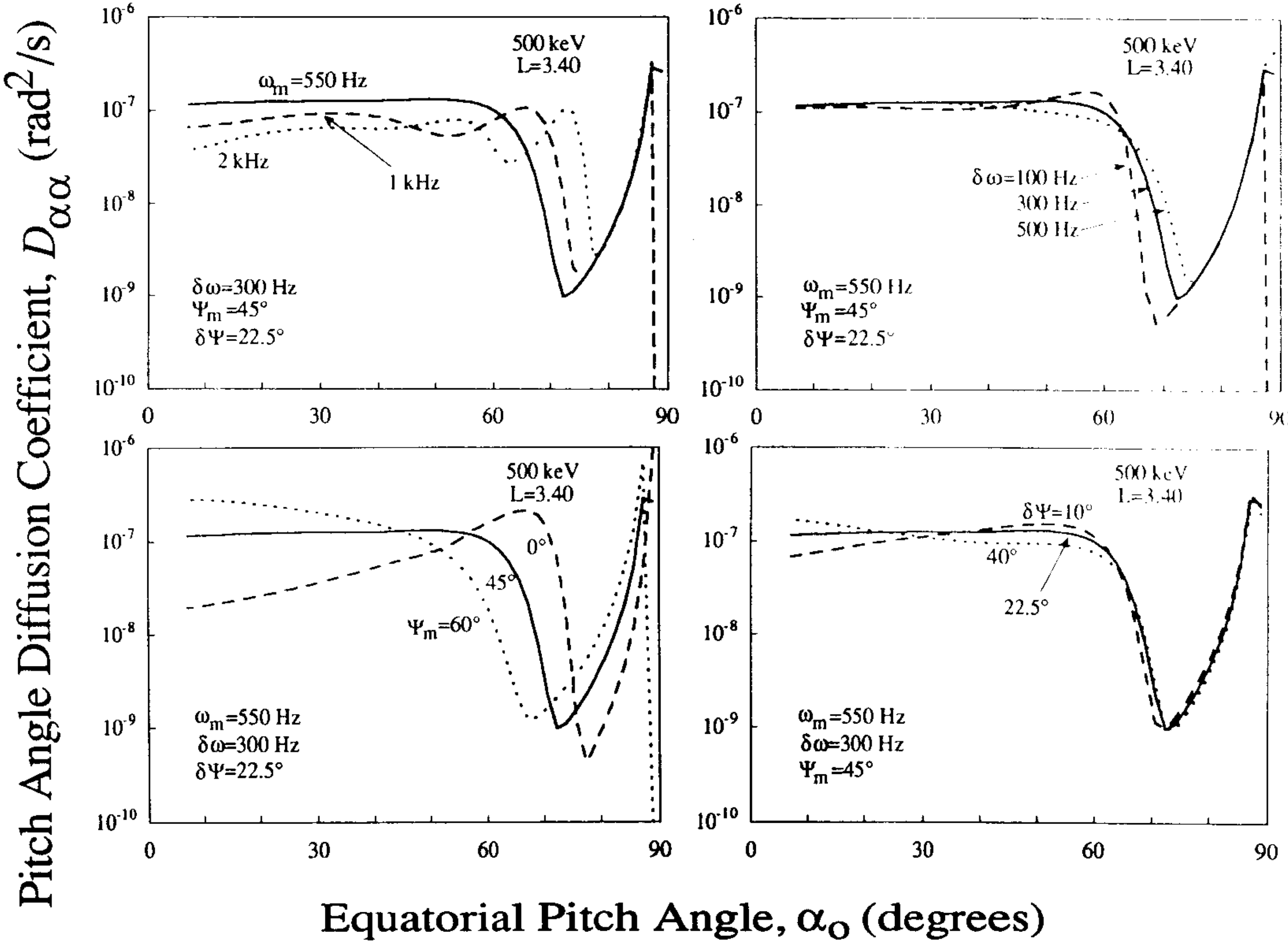
Pitch Angle Diffusion Coefficient, $D_{\alpha\alpha}$ (rad^2/s)
Equatorial Pitch Angle, α_o (degrees)
500 keV
L=3.40
ω_m=550 Hz
2 kHz
1 kHz
$\delta\omega$=300 Hz
Ψ_m=45°
$\delta\Psi$=22.5°
500 keV
L=3.40
$\delta\omega$=100 Hz
300 Hz
500 Hz
ω_m=550 Hz
Ψ_m=45°
$\delta\Psi$=22.5°
500 keV
L=3.40
0°
45°
Ψ_m=60°
ω_m=550 Hz
$\delta\omega$=300 Hz
$\delta\Psi$=22.5°
500 keV
L=3.40
$\delta\Psi$=10°
40°
22.5°
ω_m=550 Hz
$\delta\omega$=300 Hz
Ψ_m=45°

fig. 7

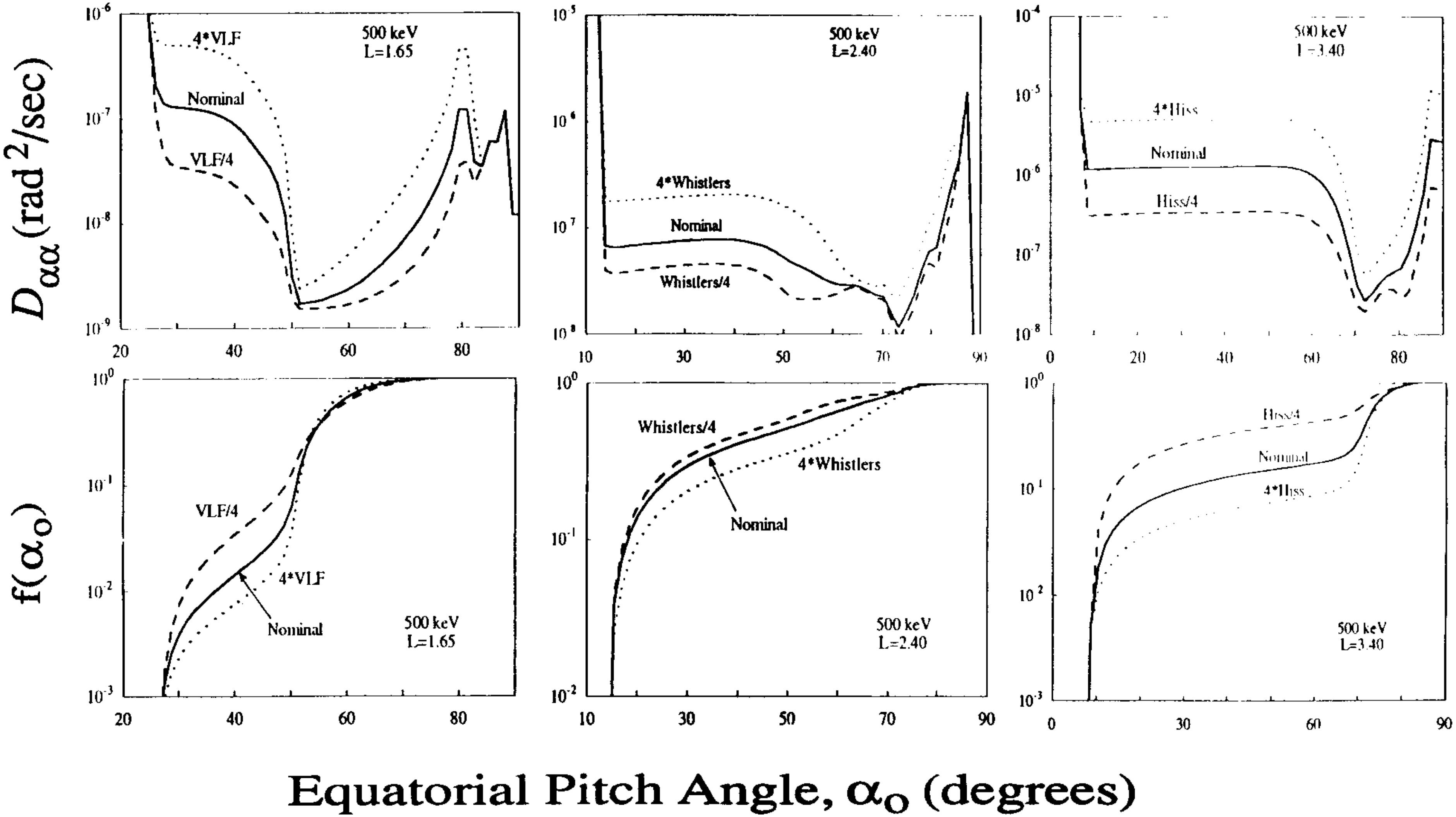

$D_{\alpha\alpha}$ (rad ^{2}/sec)
f(α_o)
500 keV
L=1.65
4*VLF
Nominal
VLF/4
500 keV
L=2.40
4*Whistlers
Nominal
Whistlers/4
500 keV
L=3.40
4*Hiss
Nominal
Hiss/4
Equatorial Pitch Angle, α_o (degrees)

Fig. 8

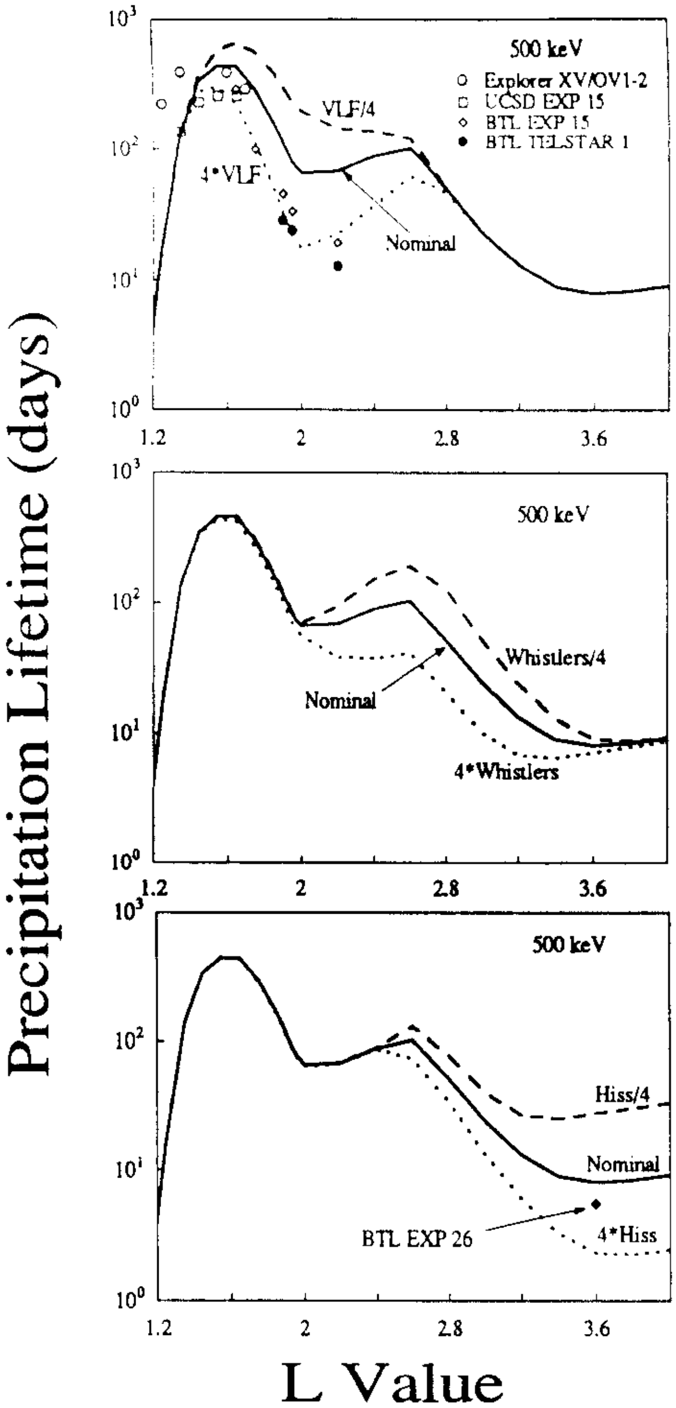
Precipitation Lifetime (days)
500 keV
Explorer XV/OV1-2
UCSD EXP 15
BTL EXP 15
BTL TELSTAR 1
VLF/4
4*VLF
Nominal
500 keV
Whistlers/4
Nominal
4*Whistlers
500 keV
Hiss/4
Nominal
BTL EXP 26
4*Hiss
L Value

F. 9

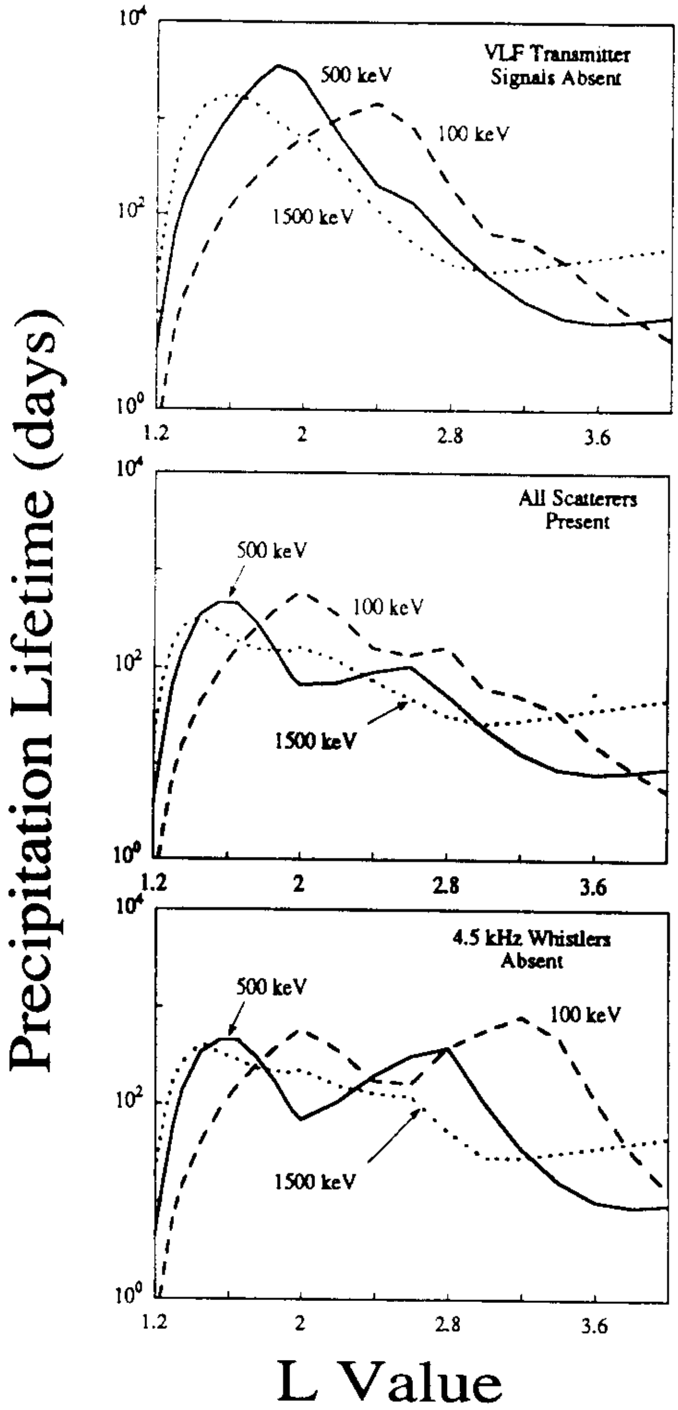
Precipitation Lifetime (days)
VLF Transmitter Signals Absent
500 keV
100 keV
1500 keV
All Scatterers Present
500 keV
100 keV
1500 keV
4.5 kHz Whistlers Absent
500 keV
100 keV
1500 keV
10^4
10^2
10^0
1.2
2
2.8
3.6
L Value

Fig. 10

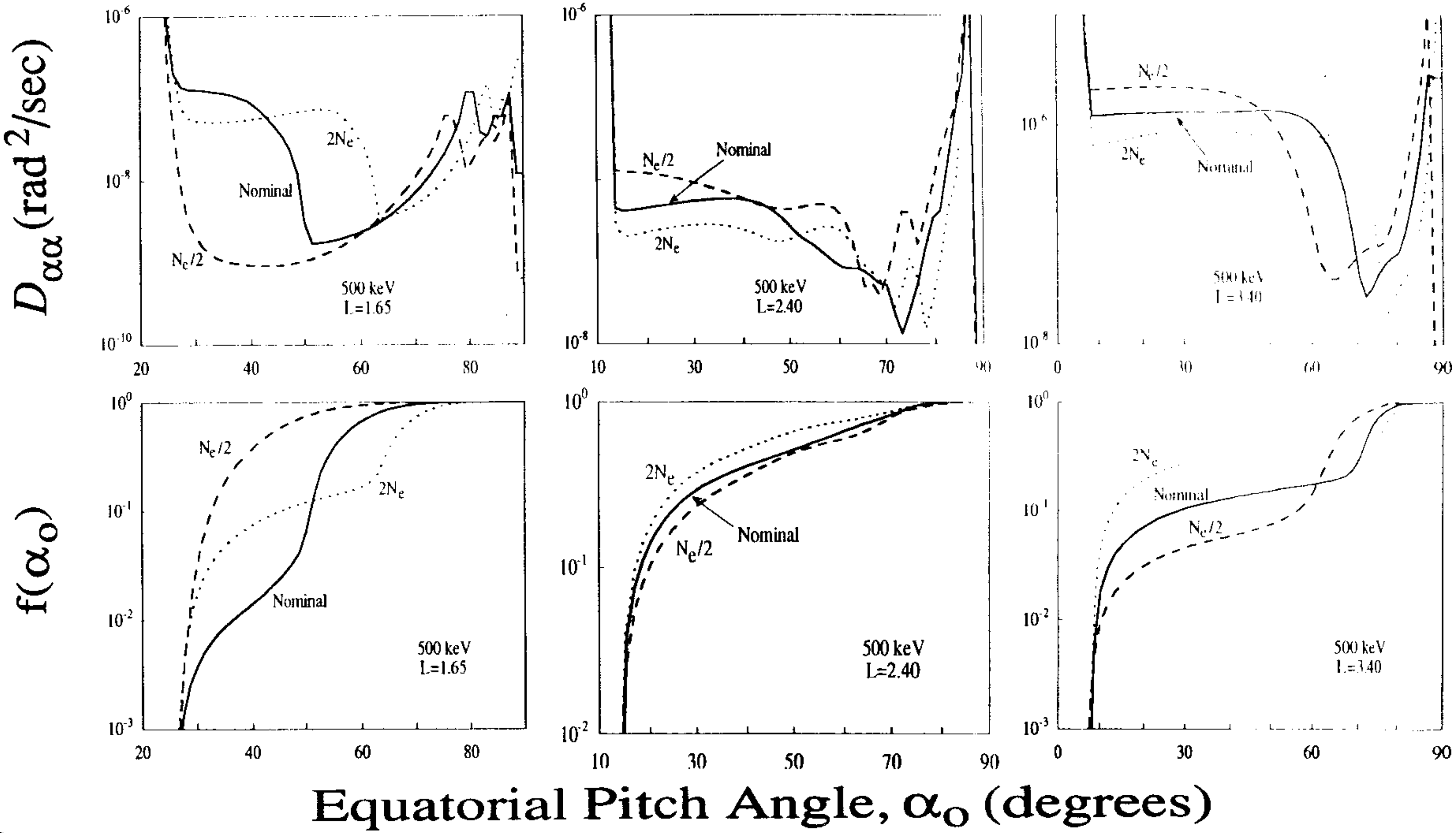

$D_{\alpha\alpha}$(rad ^{2}/sec)
$f(\alpha_o)$
Nominal
$2N_e$
$N_e/2$
500 keV
L=1.65
500 keV
L=2.40
500 keV
L=3.40
Equatorial Pitch Angle, α_o (degrees)

Fig 10

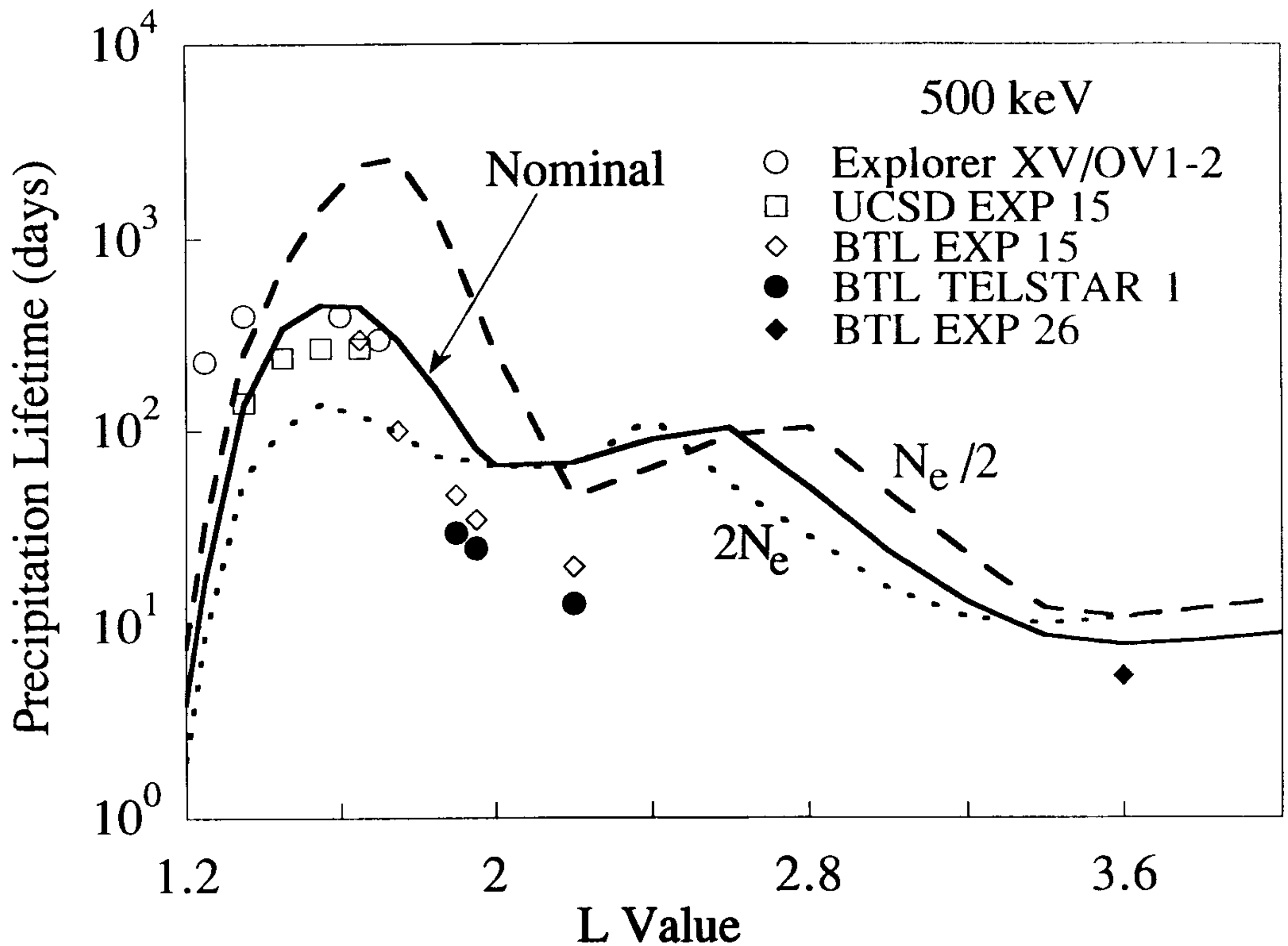
500 keV
Explorer XV/OV1-2
UCSD EXP 15
BTL EXP 15
BTL TELSTAR 1
BTL EXP 26
Nominal
$N_e/2$
$2N_e$
Precipitation Lifetime (days)
L Value
10^0
10^1
10^2
10^3
10^4
1.2
2
2.8
3.6

Fig. 12

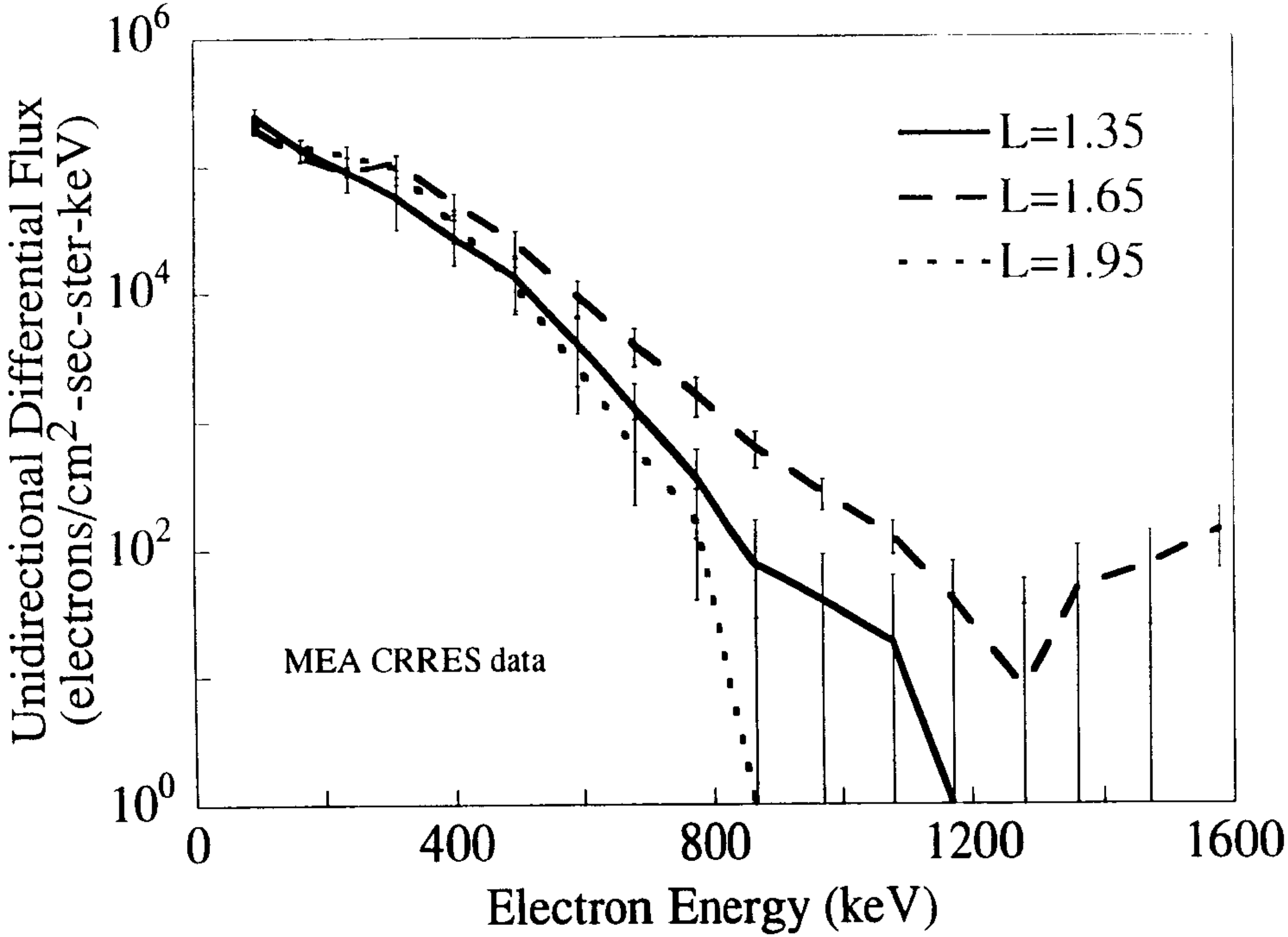

Unidirectional Differential Flux
(electrons/cm2-sec-ster-keV)
10^6
10^4
10^2
10^0
0
400
800
1200
1600
Electron Energy (keV)
L=1.35
L=1.65
L=1.95
MEA CRRES data

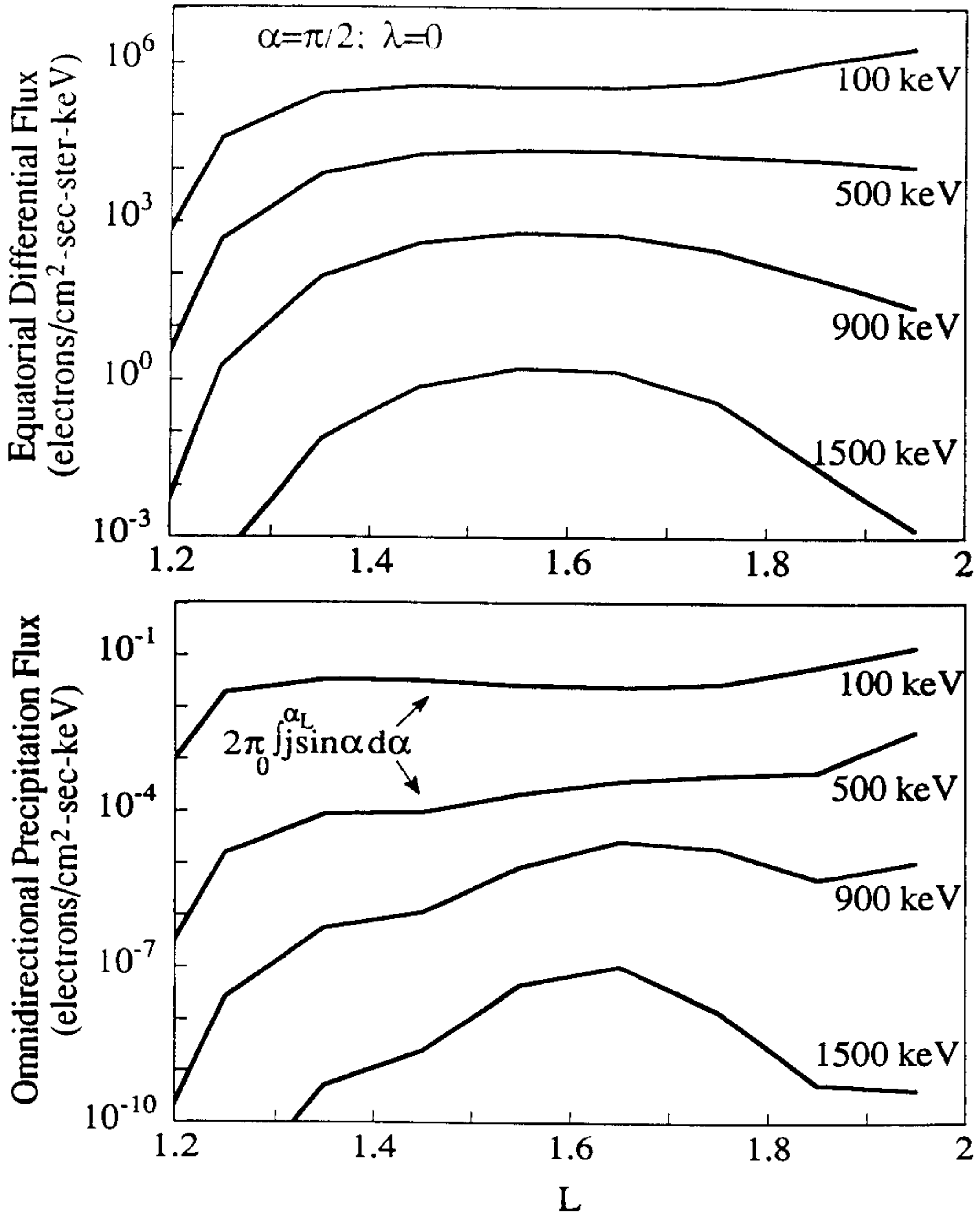
α=π/2; λ=0
Equatorial Differential Flux (electrons/cm²-sec-ster-keV)
10⁶
10³
10⁰
10⁻³
100 keV
500 keV
900 keV
1500 keV
1.2
1.4
1.6
1.8
2
Omnidirectional Precipitation Flux (electrons/cm²-sec-keV)
10⁻¹
10⁻⁴
10⁻⁷
10⁻¹⁰
2π ∫₀^{α_L} j sinα dα
100 keV
500 keV
900 keV
1500 keV
1.2
1.4
1.6
1.8
2
L

Fig 2

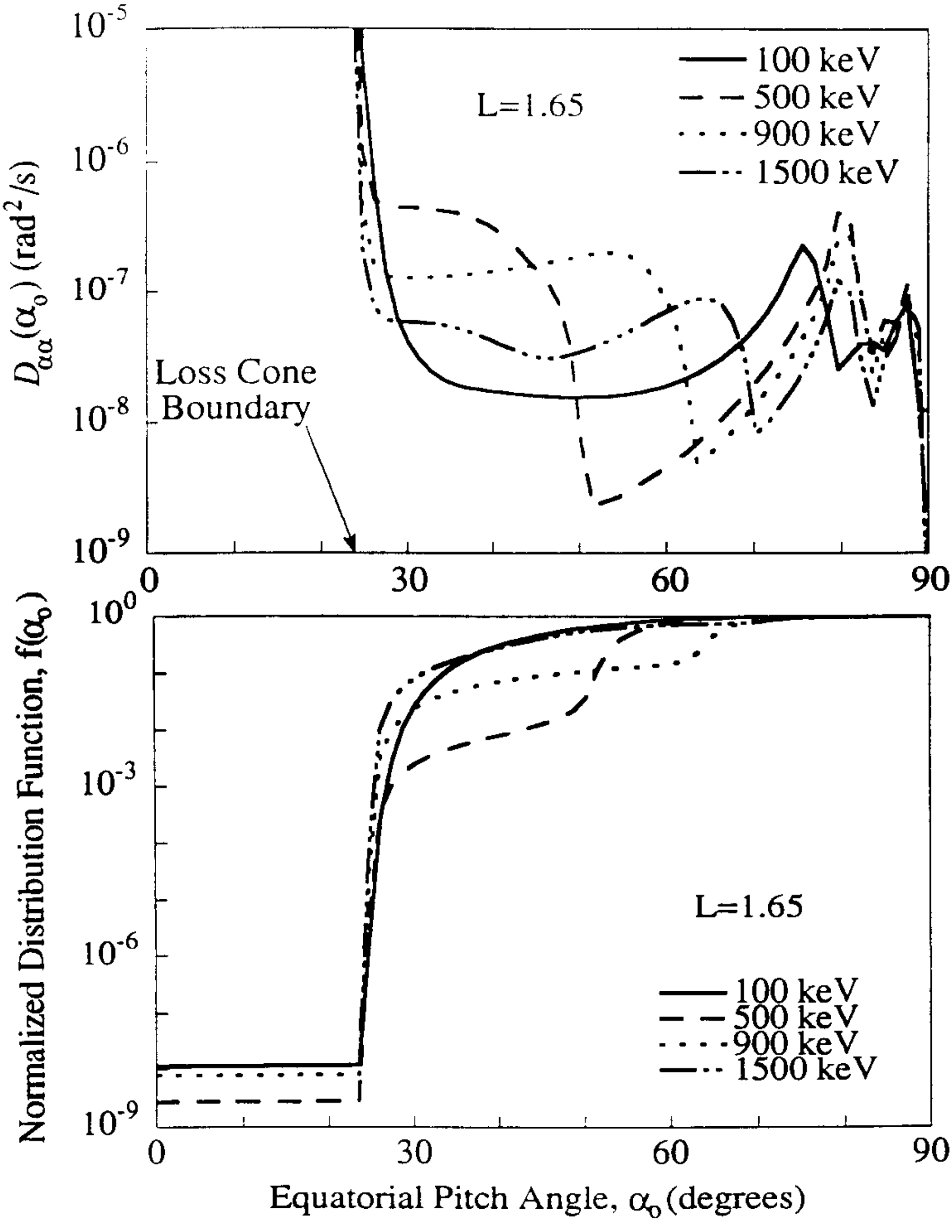

10^{-5}
10^{-6}
10^{-7}
10^{-8}
10^{-9}
$D_{\alpha\alpha}(\alpha_0)$ (rad^2/s)
L=1.65
100 keV
500 keV
900 keV
1500 keV
Loss Cone Boundary
0
30
60
90
10^0
10^{-3}
10^{-6}
10^{-9}
Normalized Distribution Function, $f(\alpha_0)$
L=1.65
100 keV
500 keV
900 keV
1500 keV
0
30
60
90
Equatorial Pitch Angle, α_0 (degrees)

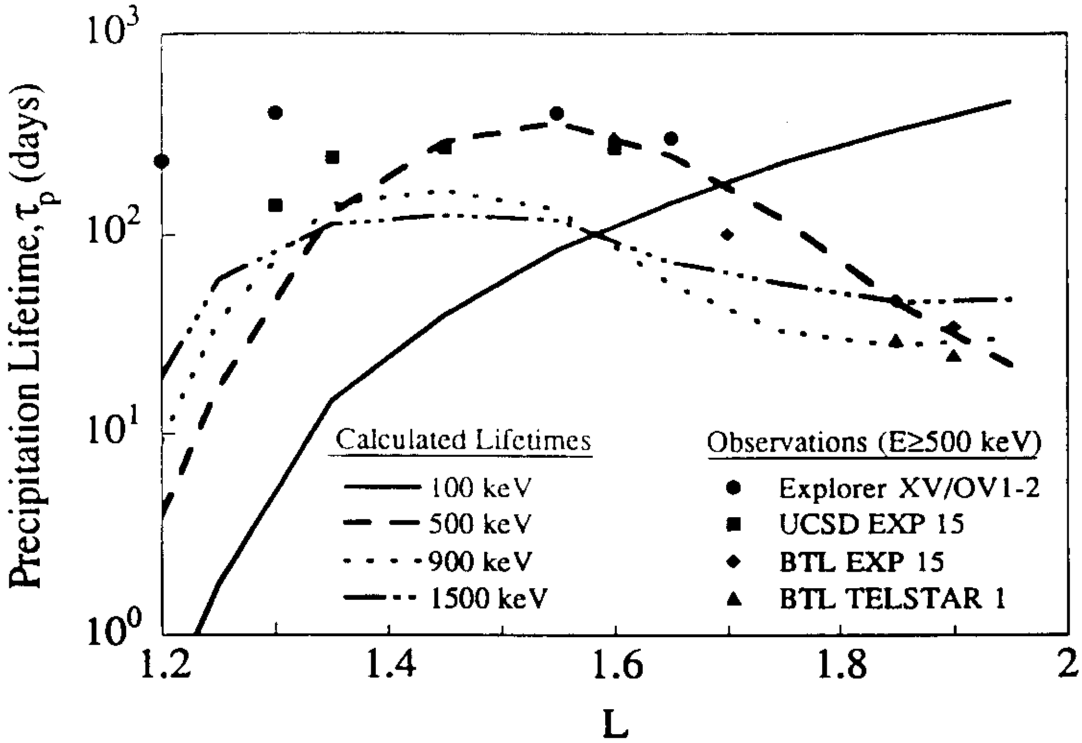

Precipitation Lifetime, τ_p (days)
10^3
10^2
10^1
10^0
1.2
1.4
1.6
1.8
2
L
Calculated Lifetimes
100 keV
500 keV
900 keV
1500 keV
Observations (E≥500 keV)
Explorer XV/OV1-2
UCSD EXP 15
BTL EXP 15
BTL TELSTAR 1

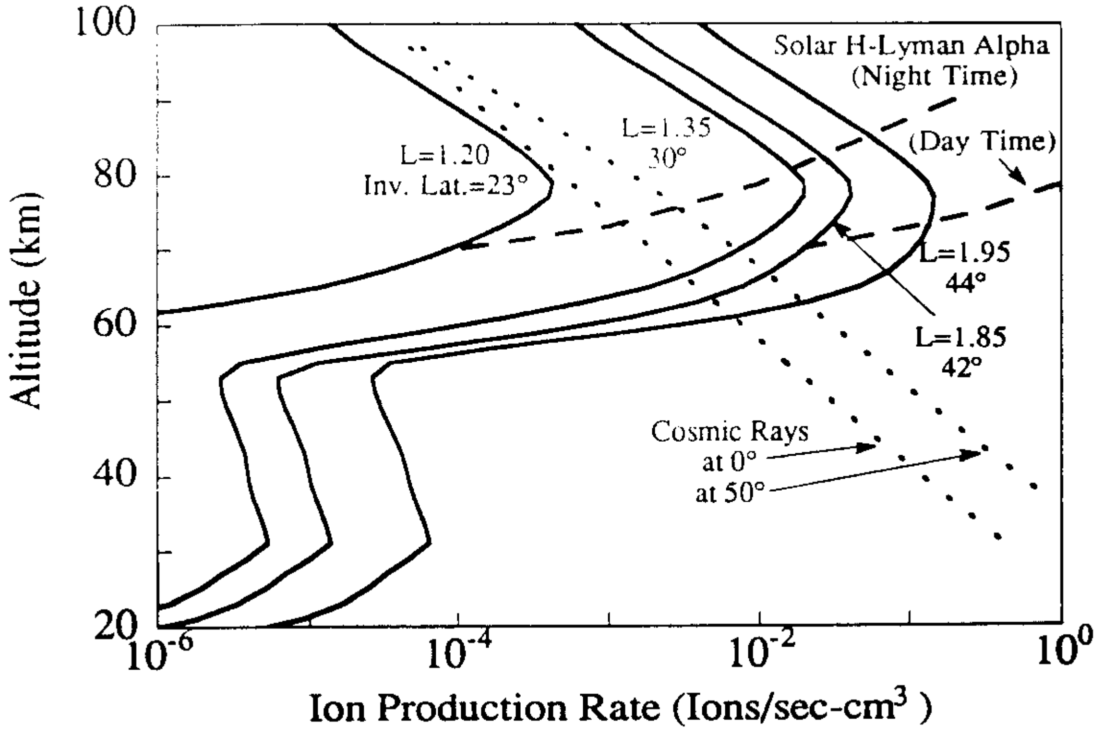
Solar H-Lyman Alpha
(Night Time)
(Day Time)
L=1.20
Inv. Lat.=23°
L=1.35
30°
L=1.95
44°
L=1.85
42°
Cosmic Rays
at 0°
at 50°
Altitude (km)
100
80
60
40
20
10-6
10-4
10-2
10^0
Ion Production Rate (Ions/sec-cm3)